

Structure–Activity Relationship Studies on a Series of 3 α -[Bis(4-fluorophenyl)methoxy]tropanes and 3 α -[Bis(4-fluorophenyl)methylamino]tropanes As Novel Atypical Dopamine Transporter (DAT) Inhibitors for the Treatment of Cocaine Use Disorders

Mu-Fa Zou,[†] Jianjing Cao,[†] Ara M. Abramyan,[†] Theresa Kopajtic,[‡] Claudio Zanettini,[†] Daryl A. Guthrie,[†] Rana Rais,[§] Barbara S. Slusher,[§] Lei Shi,[†] Claus J. Loland,^{||} and Amy Hauck Newman^{*,†}

[†]Molecular Targets and Medications Discovery Branch, National Institute on Drug Abuse—Intramural Research Program, National Institutes of Health, 333 Cassell Drive, Baltimore, Maryland 21224, United States

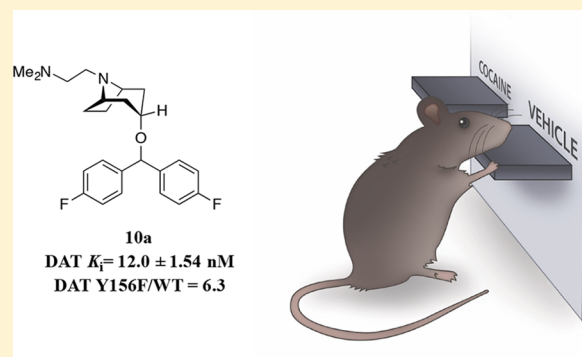
[‡]Psychobiology Section, Molecular Neuropsychiatry Research Branch, National Institute on Drug Abuse—Intramural Research Program, National Institutes of Health, 251 Bayview Boulevard, Baltimore, Maryland 21224, United States

[§]Department of Neurology, Johns Hopkins Drug Discovery, The Johns Hopkins University School of Medicine, 855 North Wolfe Street, Baltimore, Maryland 21205, United States

^{||}Molecular Faculty of Health and Medical Sciences, University of Copenhagen, DK-2200 Copenhagen, Denmark

Supporting Information

ABSTRACT: The development of medications to treat cocaine use disorders has thus far defied success, leaving this patient population without pharmacotherapeutic options. As the dopamine transporter (DAT) plays a prominent role in the reinforcing effects of cocaine that can lead to addiction, atypical DAT inhibitors have been developed that prevent cocaine from binding to DAT, but they themselves are not cocaine-like. Herein, a series of novel DAT inhibitors were synthesized, and based on its pharmacological profile, the lead compound **10a** was evaluated in phase I metabolic stability studies in mouse liver microsomes and compared to cocaine in locomotor activity and drug discrimination paradigms in mice. A molecular dynamic simulation study supported the hypothesis that atypical DAT inhibitors have similar binding poses at DAT in a conformation that differs from that of cocaine. Such differences may ultimately contribute to their unique behavioral profiles and potential for development as cocaine use disorder therapeutics.



INTRODUCTION

In 2016, the U.S. Surgeon General's report on alcohol, drugs, and health in America was entitled "Facing Addiction in America".¹ Even the title of this report commands a change in perspective from the misperception of addiction being a problem of inner cities and weak willed individuals to a severe public health matter that affects families and communities, without socioeconomic or moral bounds. Substance use disorder is a chronic medical condition, taking its toll on our public health care and judicial systems in an economically unsustainable way. As more than 20 million Americans suffer from substance use disorders, certainly, the development of prevention and treatment options as alternatives to incarceration is the appropriate and ethical solution to this escalating global problem. Although the recent opioid epidemic^{2–4} has redefined public perception of drug dependence, like cancer, addiction is not a single illness for which one treatment

modality will cure all. Hence, efforts to develop medications to treat this family of disorders must be tailored to the specific substance or substances of abuse, comorbidities with other neuropsychiatric illnesses, and ultimately individual treatment needs, which significantly increases the challenge.

Cocaine (**1**, Figure 1) is a psychostimulant and a highly addictive drug of abuse. In 2015, an estimated 1.8 million people aged 12 and older were current cocaine users.⁵ However, to date, no medication to treat cocaine abuse has proven successful.⁶ Cocaine binds to the dopamine transporter (DAT) and inhibits the reuptake of dopamine from the synapse into presynaptic neurons, resulting in an increase in extracellular dopamine levels.^{7–9} The blockade of DAT has been proposed to be the primary mechanism underlying

Received: September 29, 2017

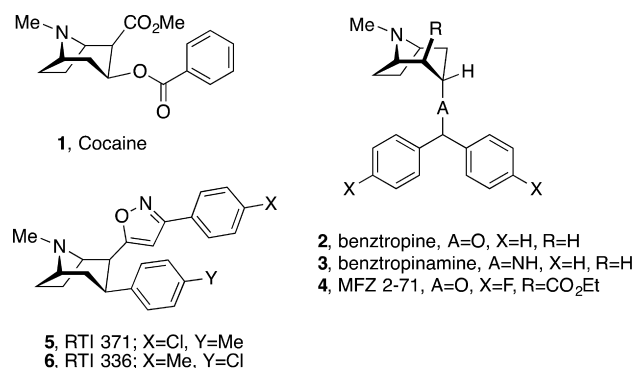


Figure 1. Chemical structures of cocaine and other tropane-based DAT inhibitors.

cocaine's psychostimulant effects and abuse liability.^{10,11} As such, DAT has been the target for the development of potential medications to treat cocaine addiction for nearly three decades, however, thus far none of the clinically available DAT inhibitors tested in this patient population has been FDA approved for treatment.^{6,12–14}

DAT belongs to the neurotransmitter:sodium symporter family. X-ray crystal structures of its homologues, such as bacterial homologue LeuT,¹⁵ drosophila DAT,^{16–18} and the human serotonin transporter (hSERT),¹⁹ as well as computational models,^{20,21} have provided a clearer picture of how the inhibitors bind and the molecular mechanisms underlying the transport of substrate.²² Significant effort has been directed toward the elucidation of the molecular structure and function of DAT as well as characterization of the binding sites of cocaine and other dopamine uptake inhibitors.²¹ However, the molecular-level details of transport inhibition by abused drugs as well as clinically therapeutic DAT inhibitors such as methylphenidate remains unknown, and this includes how chronic use affects dopamine homeostasis over time.

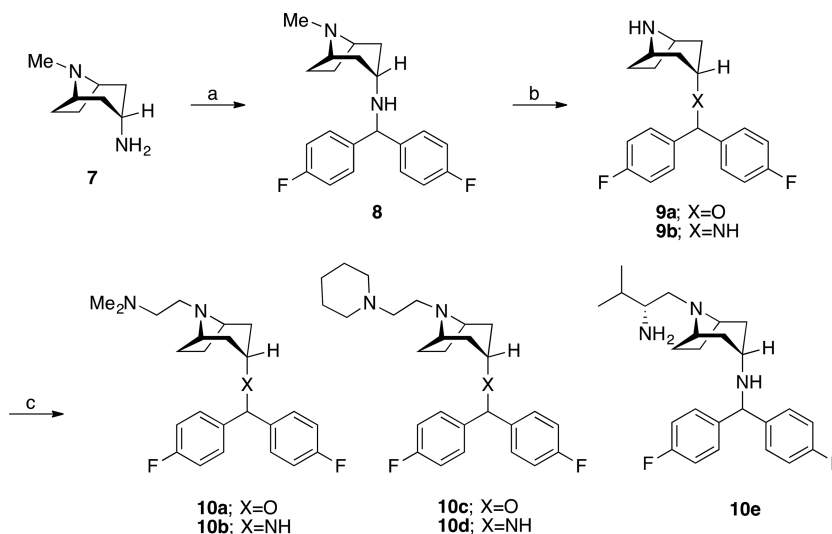
Structure–activity relationship (SAR) studies on cocaine and its 3-aryl analogues have proven useful in the identification of

structural requirements for potency and selectivity at DAT within this class of drugs.^{13,23} Most 3-aryl analogues of cocaine that have been evaluated in animal models of psychostimulant abuse have demonstrated behavioral effects and predicted abuse liability similar to cocaine. However, modification at both the 1- and 2-positions have resulted in several DAT inhibitors that do not share cocaine's behavioral profile in animal models,^{24–28} demonstrating that structural modifications on the tropane structure can affect both binding affinity to DAT and in vivo activity.

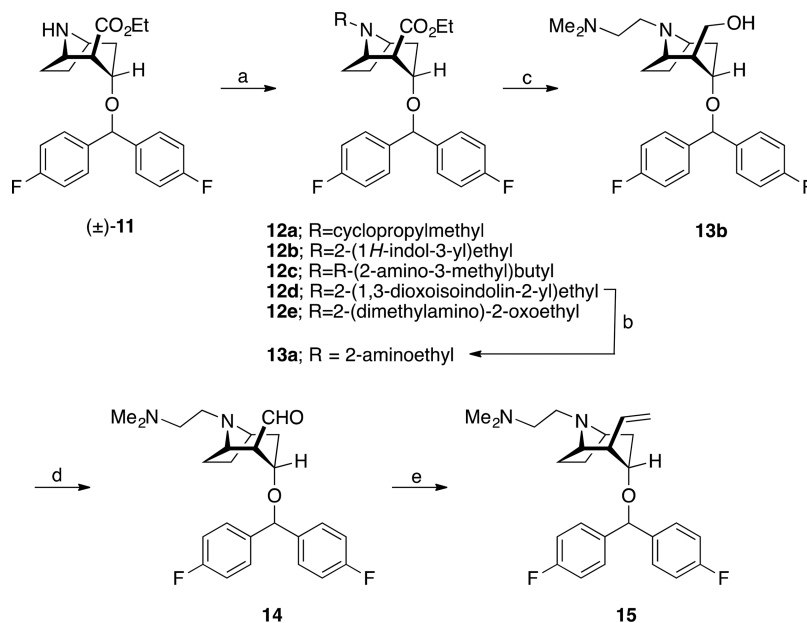
In comparison to cocaine and its 3-aryl analogues, another class of tropane-based DAT inhibitors, based on 3 α -(diphenylmethoxy)tropane (benztropine, 2, Figure 1), bind to DAT with high affinity but typically do not produce cocaine-like behavioral effects in animals.^{28,29} We have previously reported that replacement of the oxygen atom in the benztropines with a nitrogen atom results in the formation of a class of benztropinamines (e.g., compound 3, Figure 1) that bind to DAT with high affinity and selectivity.³⁰ The benztropinamines show similar SAR to the benztropines in binding to DAT as well as the other monoamine transporters such as the norepinephrine transporter and SERT.

We and others have shown that a substituent in the 2-position in the benztropine class of compounds is not necessary for binding to DAT with high affinity, in contrast to the cocaine-like structures.^{31–35} However, if there is a substituent in the 2-position, high affinity binding to DAT is conferred when this substituent is in the β -configuration; the *S*-enantiomer being the eutomer (e.g., compound 4, Figure 1), in contrast to cocaine, in which the *R*-enantiomer binds with highest DAT affinity.³⁶ Importantly, numerous studies have revealed that the benztropine-based dopamine uptake inhibitors not only have distinct structural requirements from cocaine and its 3-aryl analogues for binding to DAT but also exhibit different behavioral profiles in animal models of cocaine abuse.^{29,37–48} Indeed, these studies suggest that structurally divergent tropane-based compounds may bind differently to DAT, affected by subtle structural changes, and that the consequence

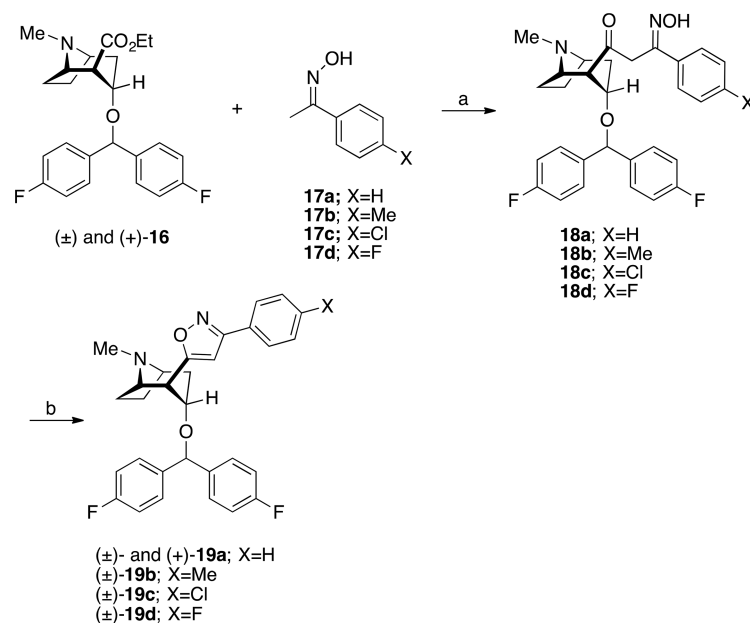
Scheme 1. Synthesis of *N*-Substituted Benztropines and Benztropinamines^a



^aReagents and conditions: (a) chlorobis(4-fluorophenyl)methane, CH₃CN, NaHCO₃, KI, overnight; (b) (i) ACE-Cl, 1,2-dichloroethane, reflux, 3 h, (ii) MeOH, reflux overnight; (c) (i) haloacetamide, CH₃CN, NaHCO₃, KI, overnight or acid chloride, 10% NaHCO₃ aqueous solution, CHCl₃, rt, 20 min, (ii) LAH, THF.

Scheme 2. Synthesis of *N*-Substituted-2 β -substituted Benzotropines^a

^aReagents and conditions: (a) RBr, DMF, 65–70 °C, overnight; (b) NH₂NH₂, EtOH, reflux, 2 h; (c) **12e**, LAH, THF, rt, overnight; (d) (COCl)₂, DMSO, Et₃N, CH₂Cl₂, –78 °C, 1 h; (e) CH₃PPh₃Br, *n*-BuLi, THF, rt, overnight.

Scheme 3. Synthesis of 2 β -Isoxazol Derivatives of Benztropine^a

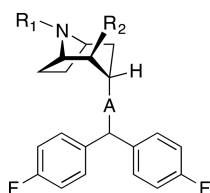
^aReagents and conditions: (a) *n*-BuLi, THF, rt, overnight; (b) HCl (3N), THF, reflux, 4 h.

of conformational changes at the transporter may be related to their *in vivo* activity profiles.^{21,49,50}

Herein, we report an extension of SAR in this class of atypical DAT inhibitors wherein compounds based on benztropine and *N*-substituted or 2-substituted benzotropines were synthesized and evaluated for binding affinities at DAT, SERT, and NET. Previous studies have shown that the isoxazol phenyltropane derivative **5** (Figure 1), an analogue of cocaine, fails to stimulate locomotor activity in mice and does not substitute in rats trained to discriminate cocaine from saline.^{27,51} In contrast, **6** (Figure 1), a constitutional isomer of **5**, does stimulate locomotion and substitutes for cocaine in rats trained to

discriminate cocaine from saline.^{27,51} Notably, **5** and **6** have similar binding affinities at DAT, SERT, and NET. As compound **5** displays an atypical behavioral profile but is reported to bind DAT in a conformation similar to cocaine, we prepared compounds **5**, **6**, and several 2 β -isoxazol-substituted compounds that are hybrids of benzotropines **2**, **4**, and the phenyltropane **5** to further investigate the effects of this substituent on the pharmacological profile of these molecules. Subsequent evaluation of a subset of DAT-selective analogues was conducted to determine their potency in inhibiting [³H]DA uptake at WT human DAT (hDAT) or [³H]-WIN35,428 binding at WT hDAT or the Y156F mutant

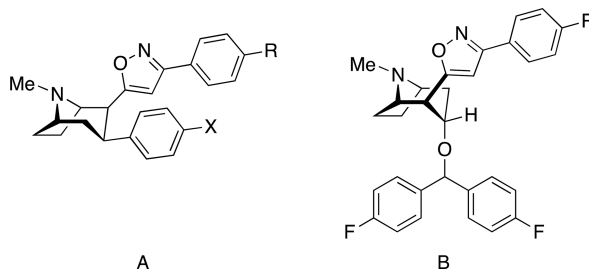
Table 1. In Vitro Binding Data on 2-Substituted or Unsubstituted 3 α -[Bis(4-fluorophenyl)methoxy]tropanes or 3 α -[Bis(4-fluorophenyl)methylamino]tropanes^a



compd	A	R ₁	R ₂	DAT K _i ± SEM (nM)	SERT K _i ± SEM (nM)	NET K _i ± SEM (nM)	hERG ^c (μM)	hERG:DAT
10a	O	CH ₂ CH ₂ N(CH ₃) ₂	H	12.0 ± 1.54	3150 ± 258	933 ± 23.6	8.23	686
10b	NH	CH ₂ CH ₂ N(CH ₃) ₂	H	14.3 ± 0.824	12000 ± 1400	4010 ± 573	5.48	383
10c	O	(CH ₂) ₂ N(CH ₂) ₃	H	13.2 ± 1.72	1460 ± 141	370 ± 53.2	5.15	390
10d	NH	(CH ₂) ₂ N(CH ₂) ₃	H	10.6 ± 1.47	3780 ± 549	612 ± 87.8	NT	
10e	NH	R-(2-amino-3-methyl)butyl	H	21.0 ± 0.634	5400 ± 673	2350 ± 269	NT	
12a	O	c-Pr-CH ₂	CO ₂ CH ₂ CH ₃	12.0 ± 1.78	3730 ± 334	555 ± 73.3	NT	
12b	O	3-ethylindole	CO ₂ CH ₂ CH ₃	26.1 ± 1.55	746 ± 57.6	1450 ± 109	14	536
12c	O	R-(2-amino-3-methyl)butyl	CO ₂ CH ₂ CH ₃	53.8 ± 3.22	1370 ± 106	4470 ± 224	NT	
13a	O	CH ₂ CH ₂ NH ₂	CO ₂ CH ₂ CH ₃	17.2 ± 0.958	5580 ± 674	862 ± 88.7	NT	
15	O	CH ₂ CH ₂ N(CH ₃) ₂	CH=CH ₂	13.5 ± 1.82	5100 ± 664	5200 ± 598	NT	
20 (GA2-50) ^b	O	R-(2-amino-3-methyl)butyl	H	13.2 ± 1.50	3870 ± 135	2130 ± 160	4.56	345
21 (GA2-99) ^b	O	CH ₂ CH ₂ NH ₂	H	5.59 ± 0.619	4600 ± 680	1420 ± 125	NT	
22 (JHW007) ^c	O	(CH ₂) ₃ CH ₃	H	9.71 ± 0.92	1350 ± 151	1490 ± 190	1.14	113
23 (PG466) ^d	N	(CH ₂) ₃ CH ₃	H	21.5 ± 2.31	2640 ± 27.6	2920 ± 209	2.35	109
24 (JHW013) ^b	O	c-Pr-CH ₂	H	24.6 ± 1.78	1420 ± 116	1640 ± 153	3.96	161
25 (GA1-69) ^b	O	3-ethylindole	H	29.2 ± 3.24	490 ± 56.4	7350 ± 934	NT	

^aEach K_i value represents data from at least three independent experiments, each performed in triplicate. K_i values were analyzed by PRISM. Binding assays are described in detail in [Experimental Methods](#). ^bBinding data previously published⁷⁰ using the same methods as described in the [Experimental Methods](#) section and included for comparison. ^cBinding data previously published³⁵ using the same methods as described in the [Experimental Methods](#) section and included for comparison. ^dBinding data previously published³⁰ using the same methods as described in the [Experimental Methods](#) section and included for comparison. ^eData from PDSP: NIMH Psychoactive Drug Screening Program using methods described.⁷¹

Table 2. In Vitro Binding Data of 2-Isoxazole-3 α -[bis(4-fluorophenyl)methoxy]tropanes^a



compd	type	X	R	DAT K _i ± SEM (nM)	SERT K _i ± SEM (nM)	NET K _i ± SEM (nM)
1, cocaine				98.1 ± 6.58	293 ± 30.0	2,120 ± 314
5 ^b	A	Me	Cl	8.55 ± 1.50	29100 ± 6330	887 ± 75.1
6 ^b	A	Cl	CH ₃	10.7 ± 1.31	23500 ± 2180	1170 ± 112
(±)-19a	B		H	60.8 ± 8.86	3830 ± 486	1100 ± 106
(S)-(+)-19a	B		H	14.4 ± 0.90	1320 ± 173	413 ± 55.8
(±)-19b	B		CH ₃	93.5 ± 11.0	4410 ± 536	2710 ± 394
(±)-19c	B		Cl	66.6 ± 2.64	756 ± 73.5	1580 ± 220
(±)-19d	B		F	69.2 ± 9.12	2990 ± 436	1640 ± 232

^aEach K_i value represents data from at least three independent experiments, each performed in triplicate. K_i values were analyzed by PRISM. Binding assays are described in detail in [Experimental Methods](#). ^bCompounds were published previously and included for comparison.^{27,51}

transiently expressed in COS7 cells. The Y156F mutation has previously been shown to adversely affect binding affinities of the atypical DAT inhibitors while having no effect on the binding affinity of cocaine.⁵²

CHEMISTRY

The aim of this first series of compounds was to extend SAR to further explore the addition of a terminal amine group in proximity to the bridgehead nitrogen of the benztropane and benzotropinamine derivatives unsubstituted in the 2-position.

The synthesis began with the reductive amination⁵³ of tropinone to give the corresponding amine **7**³⁰ (Scheme 1). Coupling of **7** with chlorobis(4-fluorophenyl)methane gave the benztropineamine **8**.³⁰ Subsequent *N*-demethylation with 1-chloroethyl chloroformate (ACE-Cl) using the Oloffson procedure gave the corresponding *N*-nor compound, **9b**. Note that **9a**⁵⁴ was previously reported and used to make the corresponding *N*-substituted benztropines. *N*-Alkylation and reduction of the intermediate amide using LAH gave benztropines (**10a** and **10c** from **9a**) and benztropineamines (**10b**, **10d**, and **10e** from **9b**) with various substitutions at the bridgehead nitrogen position.

In Scheme 2, (\pm)-*N*-nor-2 β -carboethoxy-3 α -[bis(4-fluorophenyl)methoxy]tropane (**11**)^{34,55} was alkylated to give the respective (\pm)-*N*-substituted analogues (**12a–e**). Deprotection of the phthalimide protected amine in **12d** with hydrazine resulted in the formation of amine **13a**. Reduction of **12e** with LAH gave the alcohol **13b**. Swern oxidation of **13b** formed the aldehyde **14**, which was transformed to the olefin product **15** under Wittig reaction conditions.

In Scheme 3, the 2-isoxazole analogues (**19a–d**) were prepared using a similar strategy described for **5**⁵¹ wherein the oximes **17a–d** were treated with 2 equiv of *n*-butyl lithium (*n*-BuLi) and then reacted with (\pm)-2 β -carboethoxy-3 α -bis[(4-fluorophenyl)methoxy]tropane (**16**)^{34,35,55} to give **18a–d**. Cyclization to the isoxazole analogues **19a–d** was achieved by refluxing in THF with aqueous hydrochloric acid (3 N HCl). Both intermediates **18a–d** and final products **19a–d** appeared to be unstable under these reaction conditions and started to decompose after a short time while stirring at reflux, resulting in low isolated yields of **19a–d**. (+)-**19a** was prepared from (+)-**16** using the same procedure.

RESULTS AND DISCUSSION

SAR at DAT, SERT, and NET. All final compounds (**10a–e**, **12a–c**, **13a**, **15** and **19a–d**) were evaluated for binding at DAT, SERT, and NET in rat brain membranes. Methods for the binding assays are described in the Experimental Methods section. The results of these binding studies are summarized in Tables 1 and 2 and compared to several previously reported and known DAT inhibitors **1**, **5**, **6** and **20–25**. For selected compounds, human ether-a-gogo related gene (hERG) channel data are also included.

Changes in DAT binding affinity and selectivity as a result of modifications to the benztropine structure were evaluated. In general, these novel analogues displayed low nanomolar DAT binding affinities and were selective for DAT over NET and/or SERT. We have previously shown that compounds in which the 3-position ether linkage is replaced with a secondary amine to give *N*-substituted benztropineamine analogues show similar binding affinities at DAT in comparison to their benztropine counterparts (e.g., **22** vs **23**).³⁰ In the present study, we observed the same trend as **10e** vs **20** have DAT K_i values = 21 and 13 nM, respectively. Likewise, **10b** vs **10a** and **10d** vs **10c** have similar K_i values. Hence, this substitution has no demonstrable effect on DAT binding or selectivity. When the 2-position was substituted with β -COOEt, DAT binding affinities were also not considerably affected (e.g., **12a** vs **24**, **12b** vs **25**, **12c** vs **20**, or **13a** vs **21**) as previously reported with other analogues^{34,35,55} and in contrast to the cocaine class of molecules in which the 2-position substituent is essential for high affinity binding to DAT.³⁶ Moreover, adding the 2 β -ethenyl substituent did not significantly affect DAT binding

affinity either (e.g., **10a** vs **15**). Interestingly, NET binding was significantly decreased with this substitution from K_i = 933 to 5100 nM, resulting in compound **15** being one of the most DAT-selective analogues in the series.

None of the three series of tropane-based DAT uptake inhibitors demonstrated high binding affinity at SERT or NET. In all three sets, the selectivity for DAT over SERT was consistently higher than that of DAT over NET except **12b** and **12c**, which showed higher DAT selectivity over NET than that of DAT over SERT (for **12b**, NET/DAT = 56 > SERT/DAT = 29; for **12c**, NET/DAT = 83 > SERT/DAT = 25). Compounds **10a–c** and **12b** were tested for hERG channel activity and compared to **20**, **22**, **23**, and **24**. Cardiotoxicity, in the form of drug-induced QT interval prolongation poses a significant liability for drug development. This off-target activity is primarily due to the inhibition of cardiac hERG K^+ currents.⁵⁶ Typically, a >30-fold selectivity for the drug target over hERG channel inhibition (IC_{50}) is considered sufficient to move forward with development. In this series, all compounds tested showed hERG:DAT ratios of >300, with **10a** having the highest ratio of 686.

In Table 2, the 2-isoxazole substituent, an excellent bioisostere for the methyl ester in previously described 3-aryltropane analogues,⁵¹ was explored in the benztropine class of compounds. This substituent was well tolerated in the benztropine series as well, with all analogues **19a–d** showing moderately high DAT affinities (K_i range = 61–94 nM). Notably, *S*-(+)-**19a** demonstrated the highest DAT affinity (K_i = 14 nM) in the series, comparable to the 3-aryltropane analogues **5** and **6**.⁵¹ Fluoro- or chloro- substitution on the 4-position in the (\pm)-2 β -phenylisoxazol-analogues did not affect DAT binding affinity. In general, none of the compounds demonstrated high binding affinities at NET or SERT. However, compared to the 2-isoxazol-3 α -phenyltropane compounds **5** and **6**, the 2-isoxazol-3 α -[bis(4-fluorophenyl)methoxy]tropane compounds were less selective for DAT over NET and SERT.

Molecular Pharmacology and Mutagenesis Studies.

To assess the effect of these substituents specifically on DAT function, a subset of analogues (**10a**, **10b**, **12c**, (+)-**19a**, and (\pm)-**19a**) was tested for their potency to inhibit [³H]DA uptake in COS7 cells transiently expressing human DAT. The analogues were added in a range of concentrations, typically from 0.1 nM to 100000 nM, followed by a fixed concentration of [³H]DA to allow transport. The reaction was stopped after 5 min, and the amount of [³H]DA taken up by the COS7 cells was determined by scintillation counting and plotted as a function of the concentration of added analogue. All analogues from this subset inhibited [³H]DA uptake in the K_i range of 10–1300 nM (Table 3). In this series, compounds **10a** (Figure 2A) and **10b** emerge as among the DA uptake inhibitors with highest the potency (K_i = 47 [32;68] nM and 40 [32;49] nM, respectively; mean [SEM interval], n = 4 and 3). Accordingly, their inhibition potency is >4 times higher than what we observe for cocaine (K_i = 198 [113;347] nM; mean [SEM interval], n = 3).

Although all DAT inhibitors by definition block DA uptake, they seem to do this by stabilizing DAT in different conformations. There is compelling evidence from biochemistry, molecular dynamics simulations, and structural biology^{21,49} that cocaine has a binding preference to the outward facing conformation of DAT. Here, the binding site centrally located halfway through the membrane and overlapping with the

Table 3. [³H]DA Uptake Inhibition for Selected Analogues^a

compd	DAT WT K _i (nM)	n
dopamine (k _M)	999 [891;1120]	25
1	198 [113;347]	3
5	9.7 [6.0;16]	5
6	16 [11;25]	6
10a	47 [32;68]	4
10b	40 [32;49]	3
12b	944 [401;2220]	5
12c	1050 [714;1540]	4
S-(+)- 19a	212 [162;278]	3
(±)- 19a	1300 [962;1760]	3
20	133 [96;185]	4
22	161 [132;198]	3
23	62 [49;79]	3

^aInhibition potencies (K_i values) of dopamine, cocaine, and indicated atypical inhibitors assessed as inhibition of [³H]DA uptake as depicted for **10a** in Figure 2A. Experiments are performed on COS7 cells transiently expressing DAT WT. The K_i values were calculated from the IC₅₀ values from the nonlinear regression analysis (Prism 6.0, GraphPad) using the equation $K_i = IC_{50} / (1 + (L/K_d))$, where K_d is the affinity for WIN 35,428 and L is the concentration of added [³H]WIN 35,428. Data are shown as mean [SEM interval]. All data are performed in triplicate.

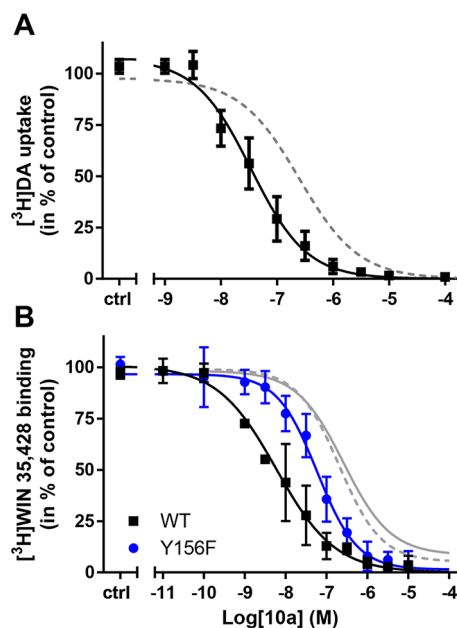


Figure 2. Pharmacological characterization and assessment of binding conformation of compound **10a**. (A) Inhibition of [³H]dopamine uptake by compound **10a** on COS7 cells transiently expressing DAT WT. Dotted line shows uptake inhibition by cocaine as determined previously.⁵² (B) Inhibition of [³H]WIN 35,428 binding by **10a** on COS7 cells transiently expressing DAT WT (black squares) or DAT Y156F (blue circles). The observed change in IC₅₀ value by the Y156F mutation is 6.3-fold, suggesting a perturbation of the binding site for **10a** by removal of the OH-group on Tyr156. Gray lines (WT, dotted; Y156F, solid) show regression analysis for comparison of similar binding experiments using cocaine performed previously,⁵² showing no significant difference in IC₅₀ values. The observed IC₅₀ values for **10a** are based on the calculated K_i values shown in Table 3. Data are means ± SEM of 3–4 experiments performed in triplicate.

binding site for dopamine^{17,21} is readily accessible from the extracellular environment. In contrast, binding of the atypical

DAT inhibitors are also competitive to dopamine binding but induce a different protein conformation in which the binding site is not as exposed to the outside.^{49,50} Thus, far, no X-ray crystal structure of DAT in complex with an atypical DAT inhibitor has been reported. However, compelling biochemical and computational evidence have proposed that, in contrast to cocaine, the binding of an atypical inhibitor to DAT is stabilized by the formation of a hydrogen bond between the OH-group of Tyr156 in TM3 and Asp79 in TM1.^{21,49,50,57,58} The two residues are located right “above” the ligand binding site and the H-bond formation could induce a closure of the extracellular gate, excluding access to the binding site from the extracellular side. In support of this hypothesis, we have previously shown that the affinity of atypical DAT inhibitors, such as the benzotropine **22** or (*R*)-modafinil, are adversely affected by the removal of the OH-group in Tyr156 (Y156F).^{21,57} In contrast, the affinity for cocaine is not affected by the Y156F mutation, suggesting that the OH-group does not contribute to cocaine binding. Accordingly, we wanted to assess whether or not compounds **10a**, **10b**, **12b**, **12c**, and (+)- and/or (±)-**19a** demonstrated an atypical DAT inhibitor binding pose by evaluating their binding affinities in DAT wild-type (WT) and the Y156F mutant (Figure 2B and Table 4). The results were compared to the effects of compounds **5**, **6**, **20**, **23**, and **25** (Table 4). Inhibition of [³H]WIN35,428 binding on COS7 cells transiently expressing WT DAT or Y156F was determined. In contrast to cocaine (Y156F:WT affinity ratio = 1.4),⁵² all the analogues showed a decrease in binding affinity for Y156F relative to DAT WT and hence Y156F:WT affinity ratios >2, with some appreciably higher. Remarkably, the benzotropinamines **10b** and **23** showed Y156F:WT affinity ratios of 20 and 15, respectively, suggesting pronounced perturbation of their binding site by the mutation. For comparison, the classical atypical DAT inhibitor, **22**, had a Y156F:WT affinity ratio of 5.5.⁵² Moreover, both compounds **5** and **6** showed Y156F:WT affinity ratios of 9.0 and 4.0, respectively.

Preclinical Evaluation of Compound 10a in Mice. Mouse Microsomal Stability Assay. On the basis of its ease of synthesis, DAT affinity (K_i = 12.0 nM), high hERG:DAT ratio (686), and Y156F:WT affinity ratio = 6.3, we chose compound **10a** as a lead molecule in this series for further evaluation. A phase I metabolic stability assay was conducted with **10a** in mouse liver microsomes. Compound **10a** was found to be remarkably stable, with 88% remaining following 1 h incubation in mouse liver microsomes, fortified with NADPH, suggesting it is highly stable to cytochrome P450 dependent metabolism (Figure 3). As a result of this promising profile, further behavioral testing was conducted in mice.

Locomotor Activity in Mice after Administration of Cocaine or 10a. In this model, as expected, cocaine dose dependently increased locomotion at doses of 20 and 40 mg/kg, producing a maximum of ≈300% of the activity counts compared to administration of vehicle (Veh vs 20 mg/kg, $q = 2.98$, $p < 0.05$; Veh vs 40 mg/kg, $q = 3.06$, $p < 0.05$; Figure 4). Compound **10a** was tested up to a dose (56 mg/kg) that produced a marked disruption of behavior indicated by suppression of locomotion to 14% of vehicle performance (Veh vs 56 mg/kg, $q = 2.97$, $p < 0.05$; Figure 4). None of the doses of **10a** significantly increased activity counts more than vehicle (Veh vs 3 mg/kg, $q = 0.162$, ns; Veh vs 10 mg/kg, $q = 0.175$, ns; Veh vs 30 mg/kg, $q = 2.27$, ns; Figure 4). The

Table 4. Assessment of DAT Inhibitor Binding Properties for Selected Analogues^a

compd	DAT WT K_i (nM)	<i>n</i>	DAT Y156F K_i (nM)	<i>n</i>	Y156F:WT affinity ratio
5 ^b	27 [21;35]	5	242 [162;362]	3	9.0
6 ^b	35 [21;54]	5	140 [129;152]	4	4.0
10a	10 [7.6;14]	3	63 [57;69]	4	6.3
10b	16 [9.7;28]	4	202 [148;274]	3	20
12b	147 [93;234]	4	1080 [913;1270]	4	7.3
12c	221 [140;349]	4	1560 [1200;2030]	4	7.1
S-(+)-19a	28 [17;47]	3	183 [114;293]	4	6.5
(±)-19a	1480 [1390;1590]	3	3490 [2790;4360]	4	2.4
20 ^b	81 [69;94]	3	307 [257;367]	5	3.8
23 ^b	24 [14;40]	4	355 [266;474]	3	15
25 ^b	253 [163;394]	4	1700 [1050;2730]	3	6.7

^aThe affinity (K_i value) for the compounds binding to DAT WT or the Y156F mutant is determined by their ability to block the binding of [³H]WIN 35,428 to COS7 cells transiently expressing DAT WT or Y156F as depicted for 10a in Figure 2B. Data were analyzed by nonlinear regression analysis using Prism 6.0 (GraphPad) and are shown as mean [SEM interval]. The K_i values were calculated from the IC_{50} values using the equation $K_i = IC_{50}/(1 + (L/K_d))$, where K_d is the affinity for WIN 35,428 and L is the concentration of added [³H]WIN 35,428. The IC_{50} values were calculated from means of pIC_{50} values and SEM interval from $pIC_{50} \pm SEM$. All data are performed in triplicate. ^bThese compounds have been previously reported.^{27,30,51,54}

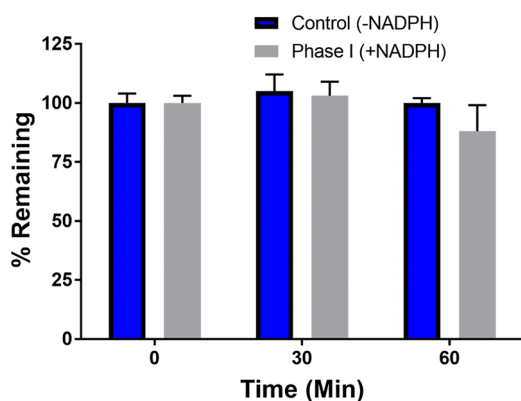


Figure 3. Phase I metabolic stability of 10a in mouse liver microsomes. 10a was incubated in mouse liver microsomes with and without NADPH (negative control), and percent remaining over time was measured via LC/MS/MS. 10a showed complete stability under all conditions. Data are presented as mean \pm SEM ($n = 3$ per time point).

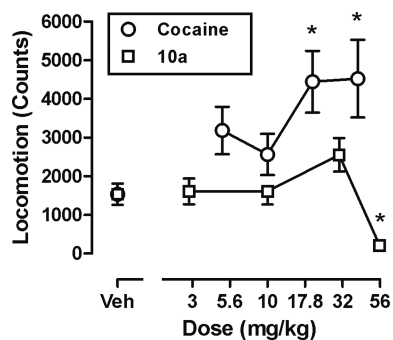


Figure 4. Effect of cocaine (5–40 mg/kg; open circles) and 10a (3–56 mg/kg; open squares) on the locomotor activity of mice during 1 h session. Ordinates: locomotor activity expressed in counts/h. Abscissa: dose in mg/kg. Each point represents the mean (\pm SEM) of six animals. Note that 10a failed to produce a significant increase in locomotor activity. Asterisks indicate a significant difference from locomotion obtained after corresponding vehicle administration (Dunnett's test; $p < 0.05$).

absence of locomotor stimulating effects by 10a indicates a pharmacological profile atypical for DAT inhibitors.

Effect of Administration of 10a in Mice Discriminating Cocaine from Saline. To further evaluate for possible cocaine-like behavioral effects, compound 10a was tested in a drug discrimination paradigm in which mice were trained to discriminate between injections (ip) of cocaine 10 mg/kg and saline. Cocaine dose dependently increased responding on the cocaine-designated lever with an ED_{50} of 3.5 mg/kg (95% CI, 2–5.1) and a maximum of >80%. In contrast, compound 10a administered 5 or 30 min before the start of the session failed to substitute for cocaine and occasioned a maximum of 23% (95% CI, –10.8–56.2, ns) cocaine lever responding (Figure 5A). None of the doses of cocaine or 10a decreased the overall group response rate below 50% of control performance, indicating that the doses tested did not markedly interfere with the execution of the behavioral task (Figure 5B). Of note, the dose of 56 mg/kg of 10a was not evaluated in the drug discrimination paradigm as it was previously shown to substantially suppress locomotor activity (Figure 4). The results of both in vivo tests in mice support an atypical behavioral profile for compound 10a as has been reported for several previously described bztropine analogues.^{40–52}

Computational Studies on 10a. On the basis of the behavioral data coupled with its Y156F:WT affinity ratio of 6.3, we went on to examine the binding pose of 10a at DAT. A molecular dynamics (MD) simulation study was conducted to test our hypothesis that the atypical DAT inhibitors have similar binding poses at DAT to one another but bind to a conformation that differs from that of cocaine. We have further hypothesized that such differences may ultimately contribute to their unique behavioral profiles and potential for development as cocaine abuse therapeutics.^{49,57}

Previously, we have characterized the isomeric preference of the classic atypical DAT inhibitor, 22, in its binding to hDAT with MD simulations in combination with Markov state model analysis.⁵⁸ We have shown the hydrogen attached to the nitrogen in the tropane ring (tNH) of 22 prefers the equatorial form in transitioning hDAT toward an inward-facing conformation.⁵⁸ With the assumption that 10a has a similar tNH isomeric preference, based on the stabilized binding pose of 22 in an inward-occluded conformation of hDAT, we selected a similar binding pose of 10a in hDAT from our

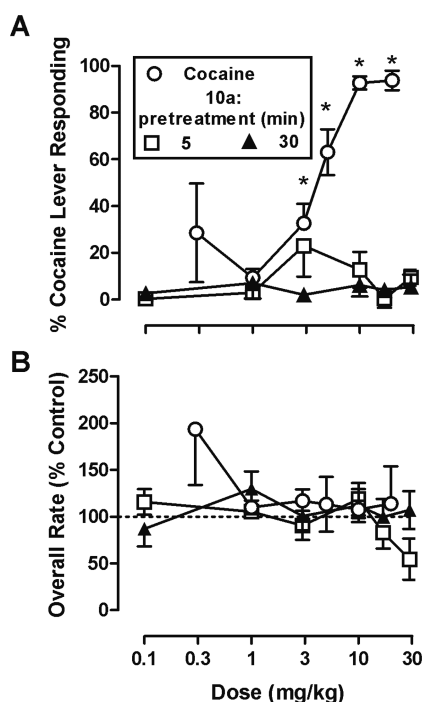


Figure 5. Effects of doses of cocaine (0.3–20 mg/kg; open circles) and 10a (0.3–30 mg/kg) given 5 min (open square) or 30 min (filled triangles) in mice trained to discriminate cocaine (10 mg/kg, ip) from vehicle. (A) Ordinates: percentage of responses emitted on the cocaine lever. (B) Ordinates: response rate expressed as percentage of response rate after saline administration. Abscissa: dose in mg/kg. Each point represents the mean (\pm SEM) of six animals. Asterisks indicate value significant different from 0 (i.e., 95% CI do not include 0). Note that 10a occasioned less than 25% cocaine lever response.

docking results and carried out MD simulations of the hDAT/10a complex (Figure 6).

As expected, our simulation results show that these two compounds share a large number of common binding residues in the central binding site of DAT (Figure 6B). The central ligand binding site can be divided into three subsites, A, B, and C,⁵⁹ in which the tropane ring and the alkyl chain of 10a and 22 are located in subsite A, whereas the two fluorophenyl rings occupy subsites B and C. Specifically, in subsite A, the charged amine of the tropane ring forms a salt bridge interaction with Asp79, while the alkyl chain forms a hydrophobic–aromatic interaction with Phe320. One of the fluorophenyl rings is in hydrophobic contact with residues from TM3 and TM8 in subsite B, whereas the other fluorophenyl ring interacts with nonpolar residues from TM3, TM6, and TM10 in subsite C. Interestingly, in comparison to the previous reported binding poses of the bntropine analogues in an outward-facing DAT model,⁵⁰ our current models of the hDAT/22⁵⁸ and hDAT/10a complexes reveal deeper binding positions of these two compounds, which likely correlate with the induced conformational transition of hDAT from the outward-facing to inward-facing state: specifically the interacting residues in subsites A and B remain largely identical, while the deeper binding positions in the inward-facing state result in interactions with residues located more intracellularly on TM3 and TM6 in subsite C. However, even in their deeper binding positions, the resulting poses are still consistent with previous mutagenesis study⁵⁰ that indicated Asn157 in TM3 is critical in interacting with one of the phenyl ring's fluorine substituent, whereas Ala480 is in close vicinity to the other fluorine, although the terminal $N(\text{CH}_3)_2$ of 10a appears to shift its pose toward Asn157 (Figure 6B,C).

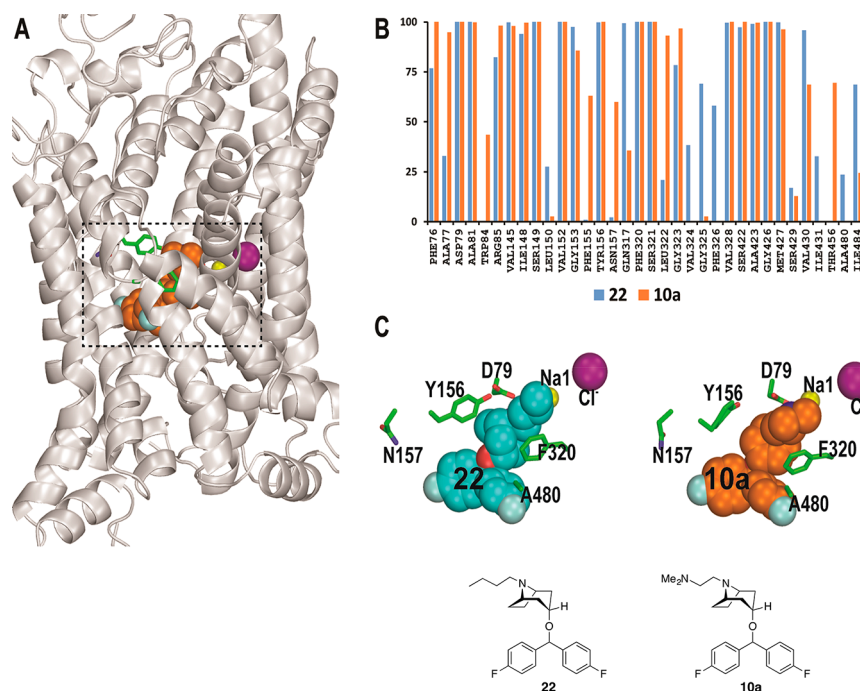


Figure 6. Molecular modeling the binding pose of 10a. (A) Side view of the hDAT/10a complex. (B) Interaction frequencies of the binding site residues (heavy atoms of which are within 5 Å of ligand heavy atoms) for the last 300 ns of each trajectory averaged for each condition. (C) A zoomed-in view of 22 and 10a binding poses, showing the hDAT residues Asn157 and Ala480 that have been previously mutated. The results in C are colored in the same way as in B.

CONCLUSION

In summary, novel dopamine uptake inhibitors based on *N*-substituted or 2 β -substituted benztropine or benztropinamines were synthesized. Binding evaluation revealed that substitution at the tropane nitrogen resulted in retention of high DAT binding affinity (K_i range = 10.6–53.8 nM) and selectivity over SERT and NET and that replacing the 3-position O with a N had no effect on the transporter binding profile of these compounds. Replacement of the 2 β -carboalkoxy group with the 2 β -isoxazole in the benztropine series resulted in a slight decrease in DAT binding affinity in the racemic group of analogues, however, *S*-(+)-**19a** demonstrated DAT affinity in the same range as the *N*-substituted analogues, as well as the previously reported isoxazole analogues from Carroll and colleagues (**5** and **6**). Interestingly, replacement of the 2 β -carboalkoxy group with an ethenyl group gave the most DAT selective analogue in the series. These data extend our previously reported SAR and confirm that the benztropines and the 3-aryl derivatives of cocaine appear to access different binding poses to DAT despite very similar binding affinities and structural similarity.

On the basis of its ease of synthesis, DAT affinity (K_i = 12.0 nM), high hERG:DAT ratio (686), and Y156F:WT affinity ratio = 6.3, we chose compound **10a** as a lead molecule in this series for further evaluation. Compound **10a** showed metabolic stability in mouse liver microsomes, with 88% remaining after 1 h, suggesting resistance to CYP dependent oxidation. Unlike cocaine, compound **10a** did not significantly increase locomotor activity and did not generalize to the cocaine discriminative stimulus in mice trained to discriminate 10 mg/kg of cocaine from saline at either a 5 or 30 min pretreatment time. These data suggest that despite being a potent DA uptake inhibitor (K_i = 47 nM), compound **10a** exhibits a profile that is consistent with an atypical DAT inhibitor. The Y156F mutant data strongly support its binding to DAT as different from that of cocaine, and the molecular dynamic simulation studies suggest that it binds similarly to the classic atypical DAT inhibitor, compound **22**. Of course, further evaluation for off-target binding affinities, pharmacokinetics, and in additional models of psychostimulant abuse will be required to validate the potential for development of **10a** as a cocaine abuse medication. Nevertheless, these data further support the atypical DAT hypothesis as a class of compounds that may have potential as pharmacotherapeutics to treat psychostimulant use disorders.

EXPERIMENTAL METHODS

Synthesis. Reaction conditions and yields were not optimized. Anhydrous solvents were purchased from Aldrich and were used without further purification except for THF, which was freshly distilled from sodium benzophenone ketyl. All other chemicals and reagents were purchased from Sigma-Aldrich Co. LLC, Combi-Blocks, TCI America, OChem Incorporation, Acros Organics, Ark Pharm, and Alfa Aesar. Unless otherwise stated, amine final products either remained as free bases or were converted into oxalate salts, typically by treating the free base in isopropanol with 1:1 molar ratio of oxalic acid in acetone. Some of the oxalate salts were recrystallized from hot methanol or a methanol–acetone solvent mixture. Spectroscopic data and yields refer to the free base. Flash chromatography was performed using silica gel (EMD Chemicals, Inc.; 230–400 mesh, 60 Å). ^1H and ^{13}C NMR spectra were acquired using a Varian Mercury Plus 400 spectrometer at 400 and 100 MHz, respectively. Chemical shifts are reported in parts-per-million (ppm) and referenced according to deuterated solvent for ^1H spectra (CDCl_3 , 7.26, or $\text{DMSO-}d_6$, 2.50) and ^{13}C

spectra (CDCl_3 , 77.2, or $\text{DMSO-}d_6$, 39.5). Gas chromatography–mass spectrometry (GC/MS) data were acquired (where obtainable) using an Agilent Technologies (Santa Clara, CA) 6890N GC equipped with an HP-5MS column (cross-linked 5% PH ME siloxane, 30 m \times 0.25 mm i.d. \times 0.25 μm film thickness) and a 5973 mass-selective ion detector in electron-impact mode. Ultrapure grade helium was used as the carrier gas at a flow rate of 1.2 mL/min. The injection port and transfer line temperatures were 250 and 280 $^\circ\text{C}$, respectively, and the oven temperature gradient used was as follows: the initial temperature (100 $^\circ\text{C}$) was held for 3 min and then increased to 295 $^\circ\text{C}$ at 15 $^\circ\text{C}/\text{min}$ over 13 min, and finally maintained at 295 $^\circ\text{C}$ for 10 min. Combustion analysis was performed by Atlantic Microlab, Inc. (Norcross, GA), and the results agree within $\pm 0.5\%$ of calculated values. Melting point determination was conducted using a Thomas–Hoover melting point apparatus and are uncorrected. On the basis of NMR and combustion data, all final compounds are $>95\%$ pure. The eluting solvent system CMA refers to $\text{CHCl}_3/\text{CH}_3\text{OH}/\text{NH}_4\text{OH}$ in the percentage of methanol indicated where NH_4OH is 1%.

8-Methyl-8-azabicyclo[3.2.1]octan-3-amine Hydrochloride (7).³⁰ To a solution of 8-methyl-8-azabicyclo[3.2.1]octan-3-one (1.0 g, 7.2 mmol) in MeOH (20 mL) was added ammonium formate (4.2 g, 67 mmol) and H_2O (2.1 mL), followed by 10% Pd/C (0.9 g, 0.8 mmol). The reaction mixture was stirred at rt overnight. The catalyst was filtered over Celite, and the filtrate was concentrated under reduced pressure. The residue was dissolved in EtOH (16 mL), and conc HCl (1.25 mL) was added dropwise to give the product as a white precipitate (1.2 g, 78% yield). ^1H NMR (400 MHz, $\text{DMSO-}d_6$) δ 10.99 (1H, br s), 8.42 (1H, s), 3.70–3.81 (2H, br s), 2.67 (1H, br s), 2.48–2.69 (5H, m), 2.02–2.25 (6H, m). GC-MS (EI) 141 (M + 1).

***N*-(Bis(4-fluorophenyl)methyl)-3,8-dimethyl-8-azabicyclo[3.2.1]octan-3-amine (8).**³⁰ A mixture of **7** (1.1 g, 5.0 mmol), chlorobis(4-fluorophenyl)methane, NaHCO_3 (2.4 g, 29 mmol), and KI (0.10 g, 0.6 mmol) in CH_3CN (100 mL) was stirred at reflux overnight at 120 $^\circ\text{C}$ in a sealed pressure bottle. After cooling to rt, the reaction mixture was filtered and the filtrate was evaporated to dryness. H_2O (100 mL) was added to the residue, followed by extraction with CH_2Cl_2 (3 \times 100 mL). The combined organic layers were dried over MgSO_4 . The solvent was removed, and the crude product was purified by flash column chromatography (90:10:1 CH_2Cl_2 :MeOH: NH_4OH) to give the product as a brown solid (1.3 g, 76% yield). GC-MS (EI) 341 (M – 1).

***N*-(Bis(4-fluorophenyl)methyl)-8-azabicyclo[3.2.1]octan-3-amine (9b).** 1-Chloroethyl chloroformate (ACE-Cl, 1.6 mL, 15 mmol) was added to the mixture of **8** (1.3 g, 3.8 mmol) and Na_2CO_3 (1.6 g, 15 mmol) in 1,2-dichloroethane (20 mL). The reaction mixture was stirred at reflux for 3 h and filtered. The filtrate was concentrated under reduced pressure, followed by addition of MeOH (20 mL) and stirring at reflux overnight to give the crude product, which was converted to the free base and purified by flash column chromatography (8:2:0.1, CHCl_3 :EtOH: NH_4OH) to give the product as a yellow oil (0.80 g, 64% yield). ^1H NMR (400 MHz, CD_3OD) δ 7.18–7.23 (4H, m), 6.94–7.00 (4H, m), 4.84–4.86 (1H, m), 3.65–3.68 (1H, s), 3.18 (1H, m), 2.77 (1H, m), 2.22–2.24 (1H, m), 2.03–2.11 (3H, m), 1.92–1.97 (2H, m), 1.58–1.68 (2H, m), 1.38–1.39 (1H, m). GC-MS (EI) 327 (M – 1).

2-(3-(Bis(4-fluorophenyl)methoxy)-8-azabicyclo[3.2.1]octan-8-yl)-*N,N*-dimethylethanamine Oxalate (10a; JJC7-043). A mixture of **9a**⁵⁴ (0.36 g, 1.1 mmol), 2-chloro-*N,N*-dimethylacetamide (0.13 g, 1.1 mmol), NaHCO_3 (0.48 g, 5.7 mmol), and KI (50 mg, 0.30 mmol) in CH_3CN (20 mL) was stirred at reflux overnight at 120 $^\circ\text{C}$ in a sealed pressure bottle. After cooling to rt, the reaction mixture was filtered and the filtrate was evaporated to dryness. H_2O (50 mL) was added to the residue, followed by extraction with CH_2Cl_2 (3 \times 50 mL). The combined organic layers were dried over MgSO_4 . The solvent was removed, and the crude product was purified by flash column chromatography (90:10:1 CH_2Cl_2 :MeOH: NH_4OH) to give the amide as a brown solid (0.35 g, 92%). ^1H NMR (400 MHz, CDCl_3) δ 7.25–7.28 (4H, m), 6.99–7.03 (4H, m), 5.40 (1H, s), 3.83 (4H, m), 3.68–3.70 (1H, m), 3.10 (1H, s), 2.95–2.97 (1H, s), 2.34–2.39 (4H, m), 2.19–2.21 (2H, m), 2.01–2.04 (2H, m). GC-MS (EI) 413 (M – 1).

Reduction of the amide to the amine, using the method described for **10e**, gave the product as a yellow oil (0.30 g, 89%), which was converted to the oxalate salt in acetone and recrystallized from hot *i*-PrOH to give the product as an orange solid; mp 165–167 °C. ¹H NMR (400 MHz, CD₃OD) δ 7.38–7.42 (4H, m), 7.03–7.08 (4H, m), 5.59 (1H, s), 3.71 (1H, m), 3.46–3.55 (2H, m), 3.31 (4H, m), 2.92 (6H, s), 2.48–2.50 (2H, m), 2.33–2.37 (2H, m), 2.21–2.24 (4H, m). ¹³C NMR (100 MHz, CD₃OD) δ 160.98, 138.14, 128.34, 128.25, 114.96, 114.74, 79.89, 79.65, 71.44, 69.45, 67.00, 61.71, 52.02, 50.25, 46.93, 43.24, 43.10, 30.52, 23.95. GC-MS (EI) 400 (M). Anal. (C₂₄H₃₀F₂N₂O·2C₂H₂O₄·2.5H₂O) C, H, N.

N-(*Bis*(4-*fluorophenyl*)methyl)-8-(2-(*dimethylamino*)ethyl)-8-azabicyclo[3.2.1]octan-3-amine Oxalate (**10b**). Compound **10b** was prepared as described for **10a** from **9b** (0.36 g, 1.1 mmol) to give the product as a yellow oil (0.28 g, 64% yield over two steps), which was converted to the oxalate salt in acetone and recrystallized from hot MeOH to give the product as a white solid; mp 152–155 °C. ¹H NMR (400 MHz, CD₃OD) δ 7.30–7.37 (4H, m), 7.02–7.08 (4H, m), 4.99–5.09 (1H, m), 3.76–3.78 (2H, m), 3.50–3.52 (1H, m), 3.29–3.35 (4H, m), 2.92–2.97 (6H, m), 2.30–2.54 (4H, m), 2.21–2.24 (2H, m), 1.94–2.08 (2H, m). ¹³C NMR (100 MHz, CD₃OD) δ 129.19, 129.15, 129.11, 129.07, 114.98, 114.76, 68.13, 63.32, 61.94, 61.40, 52.35, 46.94, 46.76, 45.54, 45.27, 42.88, 42.81, 42.57, 30.31, 25.54, 24.84, 24.56, 23.83. GC-MS (EI) 397 (M – 2). Anal. (C₂₄H₃₁F₂N₃·3C₂H₂O₄·3H₂O) C, H, N.

3-(*Bis*(4-*fluorophenyl*)methoxy)-8-(2-(*piperidin-1-yl*)ethyl)-8-azabicyclo[3.2.1]octane Oxalate (**10c**). Compound **10c** was prepared as described for **10a** from **9a** (0.33 g, 1.0 mmol) and 2-bromo-1-(*piperidin-1-yl*)ethanone (0.21 g, 1.0 mmol) to give the product as a yellow oil (0.36 g, 82% yield over two steps), which was converted to the oxalate salt and recrystallized from hot MeOH to give the product as a white solid; mp 183–184 °C. ¹H NMR (400 MHz, CD₃OD) δ 7.37–7.41 (4H, m), 7.03–7.08 (4H, m), 5.59 (1H, s), 3.67 (1H, m), 2.46–2.50 (2H, m), 3.52–3.53 (4H, m), 3.23–3.31 (6H, m), 2.23–2.33 (6H, m), 1.82–1.85 (4H, m), 1.62–1.63 (2H, m). ¹³C NMR (100 MHz, CD₃OD) δ 164.77, 163.42, 161.00, 138.14, 138.11, 128.33, 128.25, 114.97, 114.75, 79.64, 66.90, 53.53, 51.16, 23.90, 22.73, 21.14. GC-MS (EI) 440 (M). Anal. (C₂₇H₃₄F₂N₂O·2C₂H₂O₄·1.25H₂O) C, H, N.

N-(*Bis*(4-*fluorophenyl*)methyl)-8-(2-(*piperidin-1-yl*)ethyl)-8-azabicyclo[3.2.1]octan-3-amine Oxalate (**10d**). Compound **10d** was prepared as described for **10b** from **9b** (0.33 g, 1.0 mmol) and 2-bromo-1-(*piperidin-1-yl*)ethan-1-one (206 mg, 1.0 mmol) to give the product as a yellow oil (0.33 g, 75% yield over two steps), which was converted to the oxalate salt in acetone and recrystallized from hot MeOH to give the product as a white solid; mp 191–192 °C. ¹H NMR (400 MHz, CD₃OD) δ 7.32–7.38 (4H, m), 7.03–7.07 (4H, m), 5.09 (1H, s), 3.43–3.51 (4H, m), 3.19–3.34 (6H, m), 2.97 (1H, br s), 2.54–2.56 (2H, m), 2.21–2.31 (4H, m), 1.99–2.03 (2H, m), 1.81–1.84 (4H, m), 1.63 (2H, br s). ¹³C NMR (100 MHz, CD₃OD) δ 163.33, 163.23, 160.80, 138.14, 129.20, 129.12, 114.97, 114.76, 61.94, 61.49, 53.48, 51.23, 45.02, 32.65, 24.65, 22.68, 21.12. GC-MS (EI) 437 (M – 2). Anal. (C₂₇H₃₅F₂N₃·3C₂H₂O₄·1.5H₂O) C, H, N.

R-8-(2-*Amino-3-methylbutyl*)-*N*-(*bis*(4-*fluorophenyl*)methyl)-8-azabicyclo[3.2.1]octan-3-amine Oxalate (**10e**). To Fmoc-L-valine (0.50 g, 1.5 mmol) in CH₂Cl₂ (10 mL) was added SOCl₂ (1 mL). The reaction mixture was stirred at reflux for 2 h. The solvent was removed, followed by crystallization from hexane to give Fmoc-L-valine-Cl, which was added to a mixture of **9b** (0.50 g, 1.5 mmol), 10% NaHCO₃ aqueous solution (10 mL), and CHCl₃ (10 mL). The reaction mixture was stirred at rt for 20 min. The solvent was removed, and H₂O (50 mL) was added to the residue, followed by extraction with CH₂Cl₂ (3 × 50 mL). The combined organic layers were dried over MgSO₄. The solvent was removed, and the crude product was purified by flash column chromatography (90:10:1, CH₂Cl₂:MeOH:NH₄OH) to give the amide as a brown solid (400 mg, 64%). ¹H NMR (400 MHz, CDCl₃) δ 7.19–7.25 (4H, m), 6.97–7.02 (4H, m), 5.30 (1H, m), 3.25–3.28 (1H, m), 2.83–2.91 (1H, m), 1.61–2.32 (10H, m), 0.90–0.95 (6H, m, 2 × CH₃). Note: deprotection of the Fmoc group occurred during the reaction, based on the NMR data.

The amide (0.40 g, 0.94 mmol) was dissolved in THF (2.8 mL) and added dropwise to a mixture of LAH (0.07 g, 1.9 mmol) in THF (1 mL) at 0 °C and stirred overnight at rt. The mixture was quenched with H₂O (0.4 mL), 15% NaOH (0.4 mL), and H₂O (1.2 mL) successively at 0 °C. The resulting mixture was filtered and washed with THF and evaporated to dryness. The crude product was purified by flash column chromatography (eluting with 10% CMA) to give the product as a brown oil (350 mg, 90%). The free base was converted to the oxalate salt in acetone and recrystallized from hot *i*-PrOH to give the product as a white solid; mp 119–121 °C; [α]_D²⁴ +19.54 (MeOH, c 0.65). ¹H NMR (400 MHz, CD₃OD) δ 7.38–7.42 (4H, m), 7.06–7.10 (4H, m), 5.19 (1H, s), 3.43 (1H, m), 2.31 (1H, m), 2.94–3.03 (2H, m), 1.82–2.45 (10H, m), 1.01–1.04 (6H, m, 2 × CH₃). ¹³C NMR (100 MHz, CD₃OD) δ 163.49, 163.43, 161.00, 129.30, 129.21, 115.19, 114.97, 63.33, 61.89, 58.12, 53.37, 48.29, 46.94, 45.77, 29.66, 23.83, 16.68, 16.44. Anal. (C₂₅H₃₃F₂N₃·3C₂H₂O₄·0.5*i*-PrOH) C, H, N.

General Procedure for the Preparation of 12a–e from (±)-11. To a solution of *N*-nor-2-β-carboethoxy-3-α-[*bis*(4-*fluorophenyl*)methoxy]tropine (±)-**11**^{34,35,55} in DMF (5 mL/1.0 mmol of (±)-**11**) was added the bromoalkane (1.2 equiv) and K₂CO₃ (2.0 equiv). The mixture was heated to 65 °C and stirred at this temperature overnight. The mixture was then filtered and the filtrate was concentrated. The residue was diluted with H₂O (10 mL/1.0 mmol of (±)-**11**) and basified with NaHCO₃ to pH 9, and extracted with CHCl₃ (×3). The combined organic layers were dried (MgSO₄) and concentrated. The residue was purified by column chromatography (eluting with CMA) to give the product.

(±)-*N*-Cyclopropylmethyl-2-β-carboethoxy-3-α-[*bis*(4-*fluorophenyl*)methoxy]tropine (**12a**). Compound **12a** was prepared from (±)-**11** (245 mg, 0.61 mmol) and 1-bromomethylcyclopropane in 84% yield. ¹H NMR (400 MHz, CDCl₃) δ 7.32–7.21 (m, 4H), 7.06–6.93 (m, 4H), 5.34 (s, 1H), 4.18–4.04 (m, 2H), 4.00 (d, *J* = 5.2 Hz, 1H), 3.95 (d, *J* = 4.8 Hz, 1H), 3.20 (br s, 1H), 2.70 (s, 1H), 2.35 (dd, *J* = 5.2, 12.4 Hz, 1H), 2.18–1.62 (m, 8H), 1.23 (t, *J* = 7.0 Hz, 3H), 0.84–0.72 (m, 1H), 0.53–0.44 (m, 1H), 0.44–0.34 (m, 1H), 0.12–0.00 (m, 2H). ¹³C NMR (100 MHz, CDCl₃) δ 172.63, 163.26, 160.82, 138.54, 138.41, 128.40, 128.33, 115.42, 115.20, 80.31, 70.88, 60.44, 60.37, 60.18, 58.05, 51.86, 36.21, 25.87, 24.67, 14.20, 10.29, 4.37, 2.16. Anal. (C₂₇H₃₁F₂NO₃) C, H, N.

(±)-*N*-(2-(1*H*-Indol-3-yl)ethyl)-2-β-carboethoxy-3-α-[*bis*(4-*fluorophenyl*)methoxy]tropine (**12b**). Compound **12b** was prepared from (±)-**11** (265 mg, 0.66 mmol) and 2-bromoethylindole in 90% yield. ¹H NMR (400 MHz, CDCl₃) δ 7.92 (s, 1H), 7.57 (d, *J* = 8.4 Hz, 1H), 7.40 (d, *J* = 8.0 Hz, 1H), 7.30–7.24 (m, 4H), 7.17 (m, 1H), 7.09 (m, 1H), 7.04–6.96 (m, 5H), 5.36 (s, 1H), 4.10–3.98 (m, 3H), 3.23 (br s, 1H), 2.91–2.79 (m, 2H), 2.75 (s, 1H), 2.62–2.53 (m, 2H), 2.24–1.77 (m, 6H), 1.20 (t, *J* = 7.2 Hz, 3H). Anal. (C₃₃H₃₄F₂N₂O₃) C, H, N.

(±)-*N*-(2-*Amino-3-methylbutyl*)-2-β-carboethoxy-3-α-[*bis*(4-*fluorophenyl*)methoxy]tropine (**12c**). Compound **12c** was prepared from (±)-**11** (310 mg, 0.77 mmol) and 2-(Fmoc-amino)-3-methylbutyl bromide in 73% yield. ¹H NMR (400 MHz, CDCl₃) δ 7.38–7.20 (4H, m), 7.06–6.95 (4H, m), 5.33 (1H, s), 4.20–4.04 (m, 2H), 3.97 (m, 1H), 3.43 (1H, m), 3.03–2.94 (2H, m), 2.18–1.62 (10H, m), 1.24 (t, *J* = 7.0 Hz, 3H), 1.01–1.04 (m, 8H), ppm. Anal. (C₂₈H₃₆F₂N₃O₃·H₂O) C, H, N.

(±)-*N*-(2-(1,3-Dioxoisindolin-2-yl)ethyl)-2-β-carboethoxy-3-α-[*bis*(4-*fluorophenyl*)methoxy]tropine (**12d**). Compound **12d** was prepared from (±)-**11** and 2-bromoethylphthalimide in 89% yield. ¹H NMR (400 MHz, CDCl₃) δ 7.83–7.80 (m, 2H), 7.70–7.67 (m, 2H), 7.27–7.20 (m, 4H), 7.06–6.90 (m, 4H), 5.31 (s, 1H), 3.96 (m, 1H), 3.85–3.72 (m, 1H), 3.70–3.46 (m, 4H), 3.26 (br s, 1H), 2.62 (s, 1H), 2.57–2.43 (m, 2H), 2.20–1.60 (m, 6H), 1.06 (t, *J* = 7.2 Hz, 3H).

(±)-*N*-[(*N,N*-Dimethylamino)-2-oxoethyl]-2-β-carboxyethyl-3-α-[*bis*(4-*fluorophenyl*)methoxy]tropine (**12e**). Compound **12e** was prepared from (±)-**11** (355 mg, 0.88 mmol) and 2-bromo-*N,N*-dimethylacetamide (176 mg, 1.06 mmol) and purified by column chromatography (eluting with 5% CMA) in 99% yield (425 mg). ¹H NMR (400 MHz, CDCl₃) δ 7.28–7.20 (m, 4H), 7.02–6.97 (m, 4H),

5.33 (s, 1H), 4.16–4.06 (m, 1H), 3.98–3.92 (m, 2H), 3.69 (m, 1H), 3.07 (m, 1H), 3.07–3.05 (m, 2H), 3.05 (s, 3H), 2.89 (s, 3H), 2.68 (m, 1H), 2.23–2.14 (m, 1H), 2.12–1.92 (m, 4H), 1.80–1.74 (m, 1H), 1.21 (t, $J = 7.4$ Hz, 3H). GC-MS (EI) m/z 441 (M-OEt), 414 (M-CONMe₂).

(±)-*N*-(2-Amino)ethyl-2β-carboxyethyl-3α-[bis(4-fluorophenyl)methoxy]tropane (**13a**). To a solution of **12d** (242 mg, 0.42 mmol) in EtOH (6 mL) was added NH₂NH₂ (27 mg, 0.84 mmol), and the mixture was heated to reflux for 2 h. The mixture was then cooled to rt, and the white precipitate was filtered. The filtrate was concentrated. The residue was purified by column chromatography (eluting with 15% CMA) to afford the pure product in 75% yield. ¹H NMR (400 MHz, CDCl₃) δ 7.30–7.20 (m, 4H), 7.05–6.96 (m, 4H), 5.33 (s, 1H), 3.97 (m, 1H), 3.87–3.75 (m, 1H), 3.70–3.45 (m, 2H), 3.23 (br s, 1H), 2.68–2.45 (m, 5H), 2.18–1.57 (m, 6H), 1.07 (t, $J = 7.2$ Hz, 3H). ¹³C NMR (100 MHz, CDCl₃) δ 172.11, 163.48, 161.04, 138.68, 138.53, 128.63, 126.60, 115.60, 115.40, 80.43, 70.73, 63.14, 60.20, 58.81, 52.15, 51.67, 37.25, 36.01, 25.75, 25.70. Anal. (C₂₅H₃₀F₂N₂O₃·0.5H₂O) C, H, N.

(±)-*N*-(*N,N*-Dimethylamino)ethyl 2β-Hydroxymethyl-3α-[bis(4-fluorophenyl)methoxy]tropane (**13b**). To a suspension of LAH (125 mg, 3.92 mmol) in dry THF (1 mL) was added dropwise the solution of *N*-[(*N,N*-dimethylamino)-2-oxoethyl] 2β-carboxyethyl-3α-[bis(4-fluorophenyl)methoxy]tropane (**12e**) (400 mg, 0.82 mmol) in THF (4 mL) at 0 °C. The reaction mixture was allowed to warm to rt after the addition and stirred overnight. The mixture was then cooled to 0 °C, and H₂O (0.1 mL) was added slowly, followed by addition of NaOH (6N, 0.3 mL) at rt. The white solid that formed was filtered off, and the filtrate was dried (K₂CO₃) and concentrated to give the product **13b** (320 mg, 90%), which was pure by TLC and was used for the next step without further purification. ¹H NMR (400 MHz, CDCl₃) δ 7.27–7.21 (m, 4H), 7.02–6.95 (m, 4H), 5.34 (s, 1H), 3.68 (dd, $J = 3.4, 10.4$ Hz, 1H), 3.48 (dd, $J = 6.0, 10.8$ Hz, 1H), 3.42–3.35 (m, 2H), 3.15 (m, 1H), 2.52–2.44 (m, 1H), 2.43–2.37 (m, 2H), 2.34–2.26 (m, 1H), 2.22 (s, 6H), 2.14–1.80 (m, 7H).

(±)-*N*-(*N,N*-Dimethylamino)ethyl 2β-Formyl-3α-[bis(4-fluorophenyl)methoxy]tropane (**14**). To a solution of (COCl)₂ (23 μL, 0.26 mmol) in dry CH₂Cl₂ (1 mL) at –78 °C was added slowly a solution of DMSO (38 mg, 0.49 mmol) in CH₂Cl₂ (1 mL) under argon. After 30 min, a solution of alcohol (**13b**) (95 mg, 0.22 mmol) in dry CH₂Cl₂ was added and the reaction mixture was stirred for 1 h at –78 °C. Et₃N (0.14 mL, 0.99 mmol) was added, and the mixture was allowed to warm to rt, then diluted with H₂O and extracted with CHCl₃. The combined organic layers were dried (MgSO₄) and concentrated to give the crude product **9** (90 mg, 95%), which was used in the next step without purification. ¹H NMR (400 MHz, CDCl₃) δ 9.56 (s, 1H), 7.27–7.20 (m, 4H), 7.02–6.95 (m, 4H), 5.34 (s, 1H), 3.97 (m, 1H), 3.68 (m, 1H), 3.14 (m, 1H), 2.50 (m, 1H), 2.43–2.27 (m, 3H), 2.24–2.16 (m, 2H), 2.21 (s, 6H), 2.11–1.78 (m, 5H).

(±)-*N*-(*N,N*-Dimethylamino)ethyl 2β-Ethenyl-3α-[bis(4-fluorophenyl)methoxy]tropane (**15**). *n*-BuLi (0.18 mL, 1.36 M in hexane, 0.25 mmol) was added dropwise to the suspension of methytriphosphonium bromide (90 mg, 0.25 mmol) in dry THF (1 mL) at 0 °C, under argon. The resulting yellow-orange solution was stirred for 30 min before the ice–H₂O bath was removed. The crude aldehyde **14** (90 mg, 0.21 mmol) in dry THF (1 mL) was then added, and the solution was stirred at rt overnight. The reaction mixture was then diluted with H₂O (5 mL) and extracted with CHCl₃ (3 × 10 mL). The combined organic layers were dried (MgSO₄) and concentrated. The residue was purified by preparative TLC (eluting with 10% CMA) to give the product **15** (41 mg) in 46% yield. ¹H NMR (400 MHz, CDCl₃) δ 7.29–7.23 (m, 4H), 7.16–6.96 (m, 4H), 6.00 (ddd, $J = 8.2, 10.2, 17.2$ Hz, 1H), 5.36 (s, 1H), 4.93–4.83 (m, 2H), 3.27 (d, $J = 4.4$ Hz, 1H), 3.13 (m, 1H), 3.04 (m, 1H), 2.44 (m, 1H), 2.37 (m, 3H), 2.24 (s, 6H), 2.08–1.82 (m, 6H), 1.75–1.70 (m, 1H). ¹³C NMR (100 MHz, CDCl₃) δ 128.49, 128.41, 128.35, 128.26, 115.41, 115.37, 115.20, 115.16, 114.81, 80.01, 73.92, 65.11, 60.02, 50.38, 44.70, 35.63, 25.60, 25.22. GC-MS (EI) m/z 426 (M⁺). Anal. (C₂₆H₃₂F₂N₂O) C, H, N.

General Procedure for the Synthesis of 19a–d from 16. *n*-BuLi (2.0 M in hexane, 2.6 equiv) was added dropwise to the solution of oxime **17** (1.3 equiv) in dry THF at 0 °C under argon. The mixture was stirred for 2 h at rt after the addition. The reaction mixture was then cooled to 0 °C, and **16**^{34,35,55} (1 equiv) in THF was added. The mixture was allowed to warm to rt overnight. The mixture was diluted with H₂O, and the two layers were separated. The aqueous layer was extracted with CHCl₃ (×3). The combined organic layers were dried (MgSO₄) and concentrated to give the crude product **18** in almost quantitative yield, which was used in the next step without further purification.

Crude **18** was dissolved in THF (10 mL/1 mmol **18**) and 3 N HCl (2.5 equiv) was added. The mixture was heated to reflux for 4 h before it was cooled to rt. The reaction mixture was then basified with 2N NaHCO₃ solution to pH 9. The two layers were separated, and the aqueous layer was extracted with CHCl₃ (×3). The combined organic layers were dried (MgSO₄) and concentrated. The residue was purified by column chromatography (5% CMA) to give the pure products **19a–d**.

(±)-2β-[3-(3-Phenylisoxazol-5-yl)-3α-[bis(4-fluorophenyl)methoxy]tropane (**19a**). Compound **19a** was prepared from (±)-**16** and **17a** as a white solid in 18% yield; mp 158.5–160.5 °C. ¹H NMR (400 MHz, CDCl₃) δ 7.80–7.77 (m, 2H), 7.46–7.41 (m, 3H), 7.35–7.25 (m, 4H), 7.05–6.97 (m, 4H), 6.52 (s, 1H), 5.50 (s, 1H), 3.74 (d, $J = 5.2$ Hz, 1H), 3.41 (br s, 1H), 3.29 (s, 1H), 3.16 (m, 1H), 2.26 (s, 3H), 2.18–1.64 (m, 6H). ¹³C NMR (100 MHz, CDCl₃) δ 162.30, 138.08, 129.73, 129.40, 128.77, 128.75, 128.70, 128.19, 128.12, 126.78, 115.53, 115.48, 115.31, 115.27, 99.86, 80.28, 71.94, 63.48, 60.57, 45.24, 41.84, 36.56, 25.63, 24.98. Anal. (C₃₀H₂₈F₂N₂O₂) C, H, N.

S-(+)-2β-[3-(3-Phenylisoxazol-5-yl)-3α-[bis(4-fluorophenyl)methoxy]tropane (*S*-(+)-**19a**). *S*-(+)-**19a** was prepared from *S*-(+)-**16** and **17a** in 15% yield; mp 159–160.5 °C; [α]_D²⁵ 11.1° (CHCl₃, c 0.6). NMR spectra were identical to that of the racemate. Anal. (C₃₀H₂₈F₂N₂O₂) C, H, N.

(±)-2β-[3-(4-Methylphenyl)isoxazol-5-yl]-3α-[bis(4-fluorophenyl)methoxy]tropane (**19b**). Compound **19b** was prepared from (±)-**16** and **17b** as a white solid in 21% yield; mp 164–167 °C. ¹H NMR (400 MHz, CDCl₃) δ 7.67 (d, $J = 7.2$ Hz, 2H), 7.36–7.20 (m, 6H), 7.03–6.97 (m, 4H), 6.48 (s, 1H), 5.49 (s, 1H), 3.73 (d, $J = 5.4$ Hz, 1H), 3.40 (br s, 1H), 3.28 (s, 1H), 3.14 (m, 1H), 2.38 (s, 3H), 2.26 (s, 3H), 2.16–1.80 (m, 6H). ¹³C NMR (100 MHz, CDCl₃) δ 174.48, 163.43 (d, $J = 15.2$ Hz), 162.25, 160.98 (d, $J = 14.4$ Hz), 139.79, 138.10, 138.07, 137.99, 137.95, 129.44, 128.78, 128.70, 128.11, 128.19, 126.66, 126.52, 115.52, 115.47, 115.30, 115.26, 99.74, 80.25, 71.94, 63.46, 60.59, 45.24, 41.84, 36.58, 25.63, 24.99, 21.40. Anal. (C₃₁H₃₀F₂N₂O₂) C, H, N.

(±)-2β-[3-(4-Chlorophenyl)isoxazol-5-yl]-3α-[bis(4-fluorophenyl)methoxy]tropane (**19c**). Compound **19c** was prepared from (±)-**16** and **17c** as a white solid in 12% yield. ¹H NMR (400 MHz, CDCl₃) δ 7.72 (d, $J = 8.2$ Hz, 2H), 7.40 (d, $J = 8.8$ Hz, 2H), 7.33–7.28 (m, 4H), 7.04–6.98 (m, 4H), 6.50 (s, 1H), 5.49 (s, 1H), 3.72 (d, $J = 4.2$ Hz, 1H), 3.40 (br s, 1H), 3.29 (s, 1H), 3.16 (m, 1H), 2.27 (s, 3H), 2.20–1.80 (m, 6H). ¹³C NMR (100 MHz, CDCl₃) δ 174.91, 163.37 (d, $J = 13.7$ Hz), 161.33, 160.92 (d, $J = 13.6$ Hz), 138.00, 137.97, 137.90, 137.87, 135.73, 129.04, 128.75, 128.66, 128.20, 128.12, 128.06, 127.89, 115.54, 115.50, 115.33, 115.29, 99.78, 80.31, 71.84, 63.46, 60.57, 45.22, 41.81, 36.46, 25.61, 24.94. Anal. (C₃₀H₂₇ClF₂N₂O₂) C, H, N.

(±)-2β-[3-(4-Fluorophenyl)isoxazol-5-yl]-3α-[bis(4-fluorophenyl)methoxy]tropane (**19d**). Compound **19d** was prepared from (±)-**16** and **17d** as a white solid in 12% yield. ¹H NMR (400 MHz, CDCl₃) δ 7.76 (m, 2H), 7.40–7.26 (m, 6H), 7.04–6.98 (m, 4H), 6.50 (s, 1H), 5.49 (s, 1H), 3.72 (d, $J = 4.2$ Hz, 1H), 3.40 (br s, 1H), 3.29 (s, 1H), 3.16 (m, 1H), 2.27 (s, 3H), 2.20–1.80 (m, 6H). ¹³C NMR (100 MHz, CDCl₃) δ 174.91, 164.89, 163.29, 162.41, 161.38, 160.99, 138.05, 137.93, 128.75, 128.72, 128.68, 128.63, 128.20, 125.64, 125.61, 115.95, 115.73, 115.53, 115.49, 115.31, 115.28, 99.74, 80.28, 71.91, 63.47, 60.56, 45.23, 41.86, 36.54, 25.61, 24.97. Anal. (C₃₀H₂₇F₃N₂O₂) C, H, N.

Radioligand Binding Assays. DAT Binding Assay. Striata were dissected from male Sprague–Dawley rat brains (supplied on ice from

Bioreclamation (Hicksville, NY) and prepared by homogenizing tissues in 20 volumes (w/v) of ice-cold modified sucrose phosphate buffer (0.32 M sucrose, 7.74 mM Na₂HPO₄, 2.26 mM NaH₂PO₄, pH adjusted to 7.4) using a Brinkman Polytron (setting 6 for 20 s) and centrifuged at 20000 rpm for 10 min at 4 °C. The resulting pellet was resuspended in buffer, recentrifuged, and suspended in buffer again to a concentration of 10 mg/mL, original wet weight (OWW). Experiments were conducted in assay tubes containing 0.5 mL sucrose phosphate buffer, 0.5 nM [³H]WIN 35,428 (*K_d* value = 5.53, specific activity = 84 Ci/mmol; PerkinElmer Life Sciences, Waltham, MA), 1.0 mg of tissue OWW, and various concentrations of inhibitor. The reaction was started with the addition of tissue, and tubes were incubated for 120 min on ice. Nonspecific binding was determined using 100 μM cocaine HCl.

SERT Binding Assay. Membranes from frozen brain stem dissected from male Sprague–Dawley rat brains (supplied on ice from Bioreclamation, Hicksville, NY) were homogenized in 20 volumes (w/v) of 50 mM Tris buffer (120 mM NaCl and 5 mM KCl, adjusted to pH 7.4) at 25 °C using a Brinkman Polytron (at setting 6 for 20 s). The tissue was centrifuged at 20000 rpm for 10 min at 4 °C. The resulting pellet was suspended in buffer and centrifuged again. The final pellet was resuspended in cold buffer to a concentration of 15 mg/mL OWW. Experiments were conducted in assay tubes containing 0.5 mL of buffer, 1.4 nM [³H]citalopram (*K_d* value = 1.94 nM, specific activity = 83 Ci/mmol; PerkinElmer Life Sciences, Waltham, MA), 1.5 mg of brain stem tissue, and various concentrations of inhibitor. The reaction was started with the addition of the tissue, and the tubes were incubated for 60 min at rt. Nonspecific binding was determined using 10 μM fluoxetine.

NET Binding Assay. Membranes from frozen frontal cortex dissected from male Sprague–Dawley rat brains (supplied on ice from Bioreclamation, Hicksville, NY) were homogenized in 20 volumes (w/v) of 50 mM Tris buffer (120 mM NaCl and 5 mM KCl, adjusted to pH 7.4) at 25 °C using a Brinkman Polytron (at setting 6 for 20 s). The tissue was centrifuged at 20000 rpm for 10 min at 4 °C. The resulting pellet was suspended in buffer and centrifuged again. The final pellet was resuspended in cold buffer to a concentration of 80 mg/mL OWW. Experiments were conducted in assay tubes containing 0.5 mL of buffer, 0.5 nM [³H]nisoxetine (*K_d* value = 1.0 nM, specific activity = 82 Ci/mmol; PerkinElmer Life Sciences, Waltham, MA), 8 mg of frontal cortex tissue, and various concentrations of inhibitor. The reaction was started with the addition of the tissue, and the tubes were incubated for 180 min at 0–4 °C. Nonspecific binding was determined using 1 μM desipramine.

The solvent used to dissolve the various analogues of benztrorpine was typically methanol and was present at a final concentration of 5%. Extensive studies previously in this and other laboratories determined that methanol has no effect on binding at DAT and SERT. However, there is an effect of methanol on binding at NET and therefore methanol concentration was controlled in all tubes in that assay. When compounds were not soluble in methanol we used either ethanol or DMSO at final concentrations of no greater than 5 or 6%, respectively. Previous studies found no effect of either of these solvents at these concentrations on binding at any of the sites. For all three monoamine transporter binding assays, incubations were terminated by rapid filtration through Whatman GF/B filters, presoaked in 0.3% (SERT) or 0.05% (DAT, NET) polyethylenimine, using a Brandel R48 filtering manifold (Brandel Instruments Gaithersburg, Maryland). The filters were washed twice with 5 mL of cold buffer and transferred to scintillation vials. Cytoscint (MP Biomedicals, OH) (3.0 mL) was added, and the vials were counted the next day using a Beckman 6000 liquid scintillation counter (Beckman Coulter Instruments, Fullerton, California) or a Tri-Carb 2910-B liquid scintillation counter (PerkinElmer Life Sciences, MA). The *K_i* values for the benztrorpine derivatives were obtained using nonlinear least-squares regression (using GraphPad Prism Software, San Diego, CA) of the displacement data giving IC₅₀ values, from which affinities (*K_i* values) were calculated using the Cheng–Prusoff equation.⁶⁰

Molecular Pharmacology. Site-Directed Mutagenesis. Synthetic cDNA encoding the human DAT (synDAT) were subcloned into

pcDNA3 (Invitrogen, Carlsbad, CA). The Y156F mutation was introduced using QuickChange (adapted from Stratagene, La Jolla, CA) and confirmed by restriction enzyme mapping and DNA sequencing. DAT WT and Y156F cDNA containing plasmids were amplified by transformation into XL1 blue competent cells (Stratagene) and grown in LB media overnight at 37 °C in an orbital incubator (Infors) at 200 rpm. Plasmids were harvested using the maxi prep kit (Qiagen) according to the manufacturer's manual.

Cell Culture and Transfection. COS7 cells were grown in Dulbecco's Modified Eagle's Medium 041 01885 supplemented with 10% fetal calf serum, 2 mM L-glutamine, and 0.01 mg/mL gentamicin at 37 °C in 10% CO₂. DAT WT and Y156F were transiently transfected into COS7 cells with Lipo2000 (Invitrogen) according to manufacturer's manual using a cDNA:Lipo2000 ratio of 1:2.

[³H]DA Uptake Experiments. Uptake assays were performed on intact COS7 cells essentially as described⁶¹ using 3,4-[Ring-2,5,6-³H]-dihydroxyphenylethylamine ([³H]DA) (30–60 Ci/mmol) (PerkinElmer). Briefly, transfected COS7 cells were plated in 24-well dishes (10⁵ cells/well) coated with polyornithine (Sigma) to achieve an uptake level of no more than 10% of total added [³H]DA. The uptake assays were carried out 2 days after transfection in uptake buffer (UB) (25 mM HEPES, 130 mM NaCl, 5.4 mM KCl, 1.2 mM CaCl₂, 1.2 mM MgSO₄, 1 mM L-ascorbic acid, 5 mM D-glucose, and 1 μM of the catechol-*O*-methyltransferase inhibitor Ro 41-0960 (Sigma), pH 7.4). Prior to the experiment, the cells were washed once in 500 μL of UB, and the nonlabeled compound was added to the cells in the indicated concentrations in a total volume of 500 μL. The assay was initiated by the addition of 6–10 nM [³H]DA. Nonspecific uptake was determined with 1 μM nomifensine (Sigma-Aldrich). After 5 min of incubation at rt, the cells were washed twice with 500 μL of ice-cold UB, lysed in 250 μL of (24-well) 1% SDS, and left for >30 min at 37 °C on gentle shaking. All samples were transferred to 24-well counting plates (PerkinElmer, Waltham, MA), and 500 μL (24-well) of Opti-phase Hi Safe 3 scintillation fluid (PerkinElmer) was added followed by counting of the plates in a Wallac Tri-Lux β-scintillation counter (PerkinElmer). All experiments were carried out with 12 determinations of DA or inhibitor concentrations ranging from 1 nM to 1 mM performed in triplicates.

[³H]WIN35,428 Binding Experiments. Binding assays were carried out essentially as described for the uptake experiments on whole cells only using [³H]2β-carbomethoxy-3β-(4-fluorophenyl)tropane ([³H]-WIN35,428) (76–87 Ci/mmol) (PerkinElmer). Previous to the binding experiment, cells were washed once in ice cold UB and, after the addition of unlabeled compound in the indicated concentrations and [³H]WIN35,428, the reactions were incubated at 5 °C until equilibrium were obtained (>90 min). All experiments were carried out with 12 determinations with inhibitor concentration range from 1 nM to 1 mM, performed in triplicate.

Mouse Microsomal Stability Assay. Phase I metabolic stability assay was conducted in mouse liver microsomes. For phase I metabolism, the reaction was carried out with 100 mM potassium phosphate buffer, pH 7.4, in the presence of NADPH regenerating system (1.3 mM NADPH, 3.3 mM glucose 6-phosphate, 3.3 mM MgCl₂, 0.4 U/mL glucose-6-phosphate dehydrogenase, 50 μM sodium citrate). Reactions in triplicate were initiated by addition of the liver microsomes to the incubation mixture (compound final concentration was 10 μM; 0.5 mg/mL microsomes). Negative controls in the absence cofactors were carried for both to determine the specific cofactor free degradation. Compound disappearance was monitored via LC/MS/MS as described previously.⁵⁵ Briefly, chromatographic analysis was performed using an Accela ultra high-performance system consisting of an analytical pump and an autosampler coupled with TSQ Vantage mass spectrometer (Thermo Fisher Scientific Inc., Waltham MA). Separation of the analyte from potentially interfering material was achieved at ambient temperature using Agilent Eclipse Plus column (100 mm × 2.1 mm i.d.) packed with a 1.8 μm C18 stationary phase. The mobile phase used was composed of 0.1% formic acid in acetonitrile and 0.1% formic acid in H₂O with gradient elution, starting with 10% (organic), linearly increasing to 99% up to 2.5 min, maintaining at 99% (2.5–3.5 min), and reequilibrating to 10% by 4.5

min. The total run time for each analyte was 5.0 min. The mass transitions used for compound **10a** was 401.256 > 356.219 and that for internal standard is 423.110 > 207.060.

Locomotor Activity Studies in Mice. Ambulatory activity of Male Swiss Webster mice (Taconic Farms) was studied in 40 cm³ clear acrylic chambers. The acrylic chambers were placed inside monitors (Omnitech Electronics, Columbus, OH) that were equipped with light-sensitive detectors spaced 2.5 cm apart along two perpendicular walls. Mounted on the opposing walls were infrared light sources that were directed at the detectors. Counts of horizontal activity were registered each time the subject interrupted a single beam and cumulated to obtain the total of the session (1 h). Cocaine or **10a** was administered intraperitoneally (ip) at a volume of 1 mL/kg immediately before the start of the session. No habituation to the experimental chambers was provided to the animals before testing. Each dose of the test compound was studied in six mice, and mice were used only once. Drug effects were evaluated by analysis of variance (ANOVA) and subsequent Dunnett's multiple comparison test.

Drug Discrimination Studies. Experimental details are essentially identical to those described previously.⁵⁷ Sessions were conducted with male Swiss Webster mice (Taconic Farms) placed in 29.2 × 24.2 × 21 cm³ operant-conditioning chambers (modified ENV-001; MED Associates, St. Albans, VT) containing two response keys (levers requiring a downward force of 0.4 N) with pairs of green and yellow light-emitting diodes above each. A dispenser delivered 45 mg food pellets (BioServ, Frenchtown, NJ) to a tray located between the response keys, and a light was mounted near the ceiling to provide overall illumination. The chambers were located inside sound attenuated boxes that contained a white noise generator. Mice were initially trained with food reinforcement to press both levers and eventually trained to press one after cocaine (10 mg/kg, ip) and the other after saline (ip) injection. All responses produced audible clicks of a relay mounted behind the front wall of the chamber. The ratio of responses to food pellets (fixed ratio or FR) was gradually increased until, under the final conditions, the completion of 10 consecutive responses on the cocaine- or saline-appropriate lever produced food. Incorrect responses reset the FR response requirement. The right-versus left-assignments of cocaine and saline keys were counter-balanced among subjects. Subjects were injected and placed in chambers. Sessions started after a 5 min time-out period, during which lights were off and responses had no consequences other than the audible click. After the time-out, the house light was turned on until the completion of the 10-response requirement and the presentation of food. Sessions ended after 20 food presentations or 15 min, whichever occurred first, and were conducted 5 days per week, with cocaine (C) or saline (S) sessions alternating according with a CSSCSC schedule. Testing was initiated after subjects met the criteria of at least 85% cocaine- or saline-appropriate responding on four consecutive sessions (two sessions of each) over the entire session, and the first FR of the session. Test sessions were identical to training sessions with the exceptions that cocaine (0.3–20 mg/kg) or **10a** (0.1–30 mg/kg) were administered before the starting of the session and that 10 consecutive responses on either lever were reinforced. Pretreatment time for cocaine was 5 min while for **10a** was either 5 or 30 min. Straight lines were fitted to the linear portion of the dose–effect curve that included one data point below 20%, one data point above 80%, and all data points in between. Slope and intercepts were then used to derive the dose of compounds that produced 50% of cocaine lever responding (ED₅₀) and relative confidence intervals (CI). The increase in % cocaine lever response produced by doses of test compounds was not considered significant if the relative 95% CI include 0.

Molecular Docking and Dynamics Simulations. The pK_a values of the two nitrogens in **10a** were calculated using three programs (Epik and Jaguar⁶² from Schrodinger suite (release 2016-4) and Chemicalize),⁶³ which predicted pK_a values of 9.9–10.3 for the tropane nitrogen and 5.5–6.0 for the nitrogen in the alkyl chain. Thus, for our docking and MD simulations under pH 7.4, the tropane nitrogen but not the alkyl chain nitrogen was protonated. In our recent

molecular modeling and simulations of hDAT in complex with **22**, we found that the equatorial tNH isomer of **22** is the more stable isomer in the binding site of hDAT.⁵⁸ Assuming that the equatorial tNH isomer is also the stable form of **10a** in the binding site, we docked it into the central binding site of the inward-occluded hDAT model using the induced-fit docking (IFD) protocol⁶¹ implemented in the Schrodinger suite (release 2016-4). We selected a **10a** binding pose that has the lowest docking score among the poses similar to that of **22** in our established hDAT/**22** model.⁵⁸

Desmond MD systems (D. E. Shaw Research, New York, NY) with OPLS3 force field⁶⁴ was used for the MD simulations. hDAT was placed into explicit 1-palmitoyl-2-oleoyl-*sn*-glycero-3-phosphocholine lipid bilayer (POPC) using the orientation of dDAT/nortriptyline structure (PDB 4M48)⁶⁵ from the Orientation of Proteins in Membranes database.⁶⁶ Simple point charge (SPC) water model⁶⁷ was used to solvate the system, charges were neutralized, and 0.15 M NaCl was added. The total system size was ~130000 atoms. The NPγT ensemble was used with constant temperature (310 K) maintained with Langevin dynamics, 1 atm constant pressure achieved with the hybrid Nose–Hoover Langevin piston method⁶⁸ on an anisotropic flexible periodic cell, and a constant surface tension (*x–y* plane). The system was initially minimized and equilibrated with restraints on the ligand heavy atoms and protein backbone atoms, followed by production runs at 310 K with all atoms unrestrained. Four independent trajectories for each hDAT/**22** and hDAT/**10a** conditions were collected with the aggregated simulation lengths of 5.7 μs for hDAT/**22** and 6.3 μs for hDAT/**10a**.

The binding site residues were determined to be those within 5.0 Å of ligand heavy atoms within the last 300 ns of trajectories. The analysis was performed using MDTraj⁶⁹ in combination with in-house Python scripts.

■ ASSOCIATED CONTENT

📄 Supporting Information

The Supporting Information is available free of charge on the ACS Publications website at DOI: 10.1021/acs.jmedchem.7b01454.

Microanalysis data (PDF)

Representative hDAT model in complex with compound and **22** (PDB)

Representative hDAT model in complex with compound and **10a** (PDB)

SMILES molecular formula strings data (CSV)

■ AUTHOR INFORMATION

Corresponding Author

*Phone: (443) 740-2887. Fax: (443) 740-2111. E-mail: anewman@intra.nida.nih.gov.

ORCID

Rana Rais: 0000-0003-4059-2453

Barbara S. Slusher: 0000-0001-9814-4157

Amy Hauck Newman: 0000-0001-9065-4072

Notes

The authors declare no competing financial interest.

■ ACKNOWLEDGMENTS

Lone Rosenquist is thanked for excellent technical assistance. Support for this research was provided to A.H.N., M.F.Z., J.C., T.K., J.K., A.M.A., D.A.G., and L.S. by the National Institute on Drug Abuse—Intramural Research Program (Z1A DA000389 21). C.J.L. is supported by the Danish Council for Independent Research (0602-02100B and 4183-00581). Care of the animals was in accordance with the guidelines of the National Institutes of Health and the National Institute on Drug Abuse Intramural

Research Program Animal Care and Use Program, which is fully accredited by AAALAC International.

■ ABBREVIATIONS USED

DA, dopamine; DAT, dopamine transporter; SERT, serotonin transporter; NET, norepinephrine transporter; IA, inactive; ND, not determined

■ REFERENCES

- (1) *Facing Addiction in America: The Surgeon General's Report on Alcohol, Drugs, and Health.*, U.S. Department of Health and Human Services (HHS), Office of the Surgeon General: Washington, DC, November 2016.
- (2) Volkow, N. D.; McLellan, A. T. Opioid Abuse in Chronic Pain-Misconceptions and Mitigation Strategies. *N. Engl. J. Med.* **2016**, *374*, 1253–1263.
- (3) Compton, W. M.; Volkow, N. D. Major Increases in Opioid Analgesic Abuse in the United States: Concerns and Strategies. *Drug Alcohol Depend.* **2006**, *81*, 103–107.
- (4) Compton, W. M.; Jones, C. M.; Baldwin, G. T. Relationship Between Nonmedical Prescription-Opioid Use and Heroin Use. *N. Engl. J. Med.* **2016**, *374*, 154–163.
- (5) *2015 National Survey on Drug Use and Health: Detailed Tables*; Center for Behavioral Health Statistics and Quality, Substance Abuse and Mental Health Services Administration: Rockville, MD, 2016.
- (6) Czoty, P. W.; Stoops, W. W.; Rush, C. R. Evaluation of the “Pipeline” for Development of Medications for Cocaine Use Disorder: A Review of Translational Preclinical, Human Laboratory, and Clinical Trial Research. *Pharmacol. Rev.* **2016**, *68*, 533–562.
- (7) Pharmacological Aspects of Drug Dependence: Toward an Integrated Neurobehavioral Approach. In *Handbook of Experimental Pharmacology*; Schuster, C. R., Kuhar, M. J., Eds.; Springer: New York, 1996; Vol. 118.
- (8) Schmitt, K. C.; Reith, M. E. A. Regulation of the Dopamine Transporter. *Ann. N. Y. Acad. Sci.* **2010**, *1187*, 316–340.
- (9) Wood, S.; Sage, J. R.; Shuman, T.; Anagnostaras, S. G. Psychostimulants and Cognition: A Continuum of Behavioral and Cognitive Activation. *Pharmacol. Rev.* **2014**, *66*, 193–221.
- (10) Ritz, M. C.; Lamb, R. J.; Goldberg, S. R.; Kuhar, M. J. Cocaine Receptors on Dopamine Transporters are Related to Self-Administration of Cocaine. *Science* **1987**, *237*, 1219–1223.
- (11) Giros, B.; Jaber, M.; Jones, S. R.; Wightman, R. M.; Caron, M. G. Hyperlocomotion and Indifference to Cocaine and Amphetamine in Mice Lacking the Dopamine Transporter. *Nature* **1996**, *379*, 606–612.
- (12) Newman, A. H.; Kulkarni, S. Probes for the Dopamine Transporter: New Leads Toward a Cocaine-Abuse Therapeutic – A Focus on Analogues of Benzotropine and Rimcazole. *Med. Res. Rev.* **2002**, *22*, 429–464.
- (13) Carroll, F. I. 2002 Medicinal Chemistry Division Award Address: Monoamine Transporters and Opioid Receptors: Targets for Addiction Therapy. *J. Med. Chem.* **2003**, *46*, 1775–1794.
- (14) Dutta, A. K.; Zhang, S.; Kolhatkar, R.; Reith, M. E. A. Dopamine Transporter as Target for Drug Development of Cocaine Dependence Medications. *Eur. J. Pharmacol.* **2003**, *479*, 93–106.
- (15) Yamashita, A.; Singh, S. K.; Kawate, T.; Jin, Y.; Gouaux, E. Crystal Structure of a Bacterial Homologue of Na⁺/Cl⁻-Dependent Neurotransmitter Transporters. *Nature* **2005**, *437*, 215–223.
- (16) Penmatsa, A.; Wang, K. H.; Gouaux, E. X-ray Structure of Dopamine Transporter Elucidates Antidepressant Mechanism. *Nature* **2013**, *503*, 85–90.
- (17) Wang, K. H.; Penmatsa, A.; Gouaux, E. Neurotransmitter and Psychostimulant Recognition by the Dopamine Transporter. *Nature* **2015**, *521*, 322–327.
- (18) Penmatsa, A.; Wang, K. H.; Gouaux, E. X-ray Structures of Drosophila Dopamine Transporter in Complex with Nisoxetine and Reboxetine. *Nat. Struct. Mol. Biol.* **2015**, *22*, 506–508.
- (19) Coleman, J. A.; Green, E. M.; Gouaux, E. X-ray Structures and Mechanism of the Human Serotonin Transporter. *Nature* **2016**, *532*, 334–339.
- (20) Davis, B. A.; Nagarajan, A.; Forrest, L. R.; Singh, S. K. Mechanism of Paroxetine (Paxil) Inhibition of the Serotonin Transporter. *Sci. Rep.* **2016**, *6*, 23789.
- (21) Beuming, T.; Kniazeff, J.; Bergmann, M. L.; Shi, L.; Gracia, L.; Raniszewska, K.; Newman, A. H.; Javitch, J. A.; Weinstein, H.; Gether, U.; Loland, C. J. The Binding Sites for Cocaine and Dopamine in the Dopamine Transporter Overlap. *Nat. Neurosci.* **2008**, *11*, 780–789.
- (22) Loland, C. J. The Use of LeuT as a Model in Elucidating Binding Sites for Substrates and Inhibitors in Neurotransmitter Transporters. *Biochim. Biophys. Acta, Gen. Subj.* **2015**, *1850*, 500–510.
- (23) Runyon, S. P.; Carroll, F. I. Dopamine Transporter Ligands: Recent Developments and Therapeutic Potential. *Curr. Top. Med. Chem.* **2006**, *6*, 1825–1843.
- (24) Reith, M. E.; Ali, S.; Hashim, A.; Sheikh, I. S.; Theddu, N.; Gaddiraju, N. V.; Mehrotra, S.; Schmitt, K. C.; Murray, T. F.; Sershen, H.; Unterwald, E. M.; Davis, F. A. Novel C-1 Substituted Cocaine Analogs Unlike Cocaine or Benzotropine. *J. Pharmacol. Exp. Ther.* **2012**, *343*, 413–425.
- (25) Hong, W. C.; Kopajtic, T. A.; Xu, L.; Lomenzo, S. A.; Jean, B.; Madura, J. D.; Surratt, C. K.; Trudell, M. L.; Katz, J. L. 2-Substituted 3β-Aryltropane Cocaine Analogs Produce Atypical Effects without Inducing Inward-Facing Dopamine Transporter Conformations. *J. Pharmacol. Exp. Ther.* **2016**, *356*, 624–634.
- (26) Carroll, F. I.; Runyon, S. P.; Abraham, P.; Navarro, H.; Kuhar, M. J.; Pollard, G. T.; Howard, J. L. Monoamine Transporter Binding, Locomotor Activity, and Drug Discrimination Properties of 3-(4-Substituted-Phenyl)tropane-2-Carboxylic Acid Methyl Ester Isomers. *J. Med. Chem.* **2004**, *47*, 6401–6409.
- (27) Hiranita, T.; Wilkinson, D. S.; Hong, W. C.; Zou, M.-F.; Kopajtic, T. A.; Soto, P. L.; Lupica, C. R.; Newman, A. H.; Katz, J. L. 2-Isoxazol-3-Phenyltropane Derivatives of Cocaine: Molecular and Atypical System Effects at the Dopamine Transporter. *J. Pharmacol. Exp. Ther.* **2014**, *349*, 297–309. Hiranita, T.; Wilkinson, D. S.; Hong, W. C.; Zou, M.-F.; Kopajtic, T. A.; Soto, P. L.; Lupica, C. R.; Newman, A. H.; Katz, J. L. Correction to “2-Isoxazol-3-Phenyltropane Derivatives of Cocaine: Molecular and Atypical System Effects at the Dopamine Transporter”. *J. Pharmacol. Exp. Ther.* **2014**, *349*, 534.
- (28) Reith, M. E.; Blough, B. E.; Hong, W. C.; Jones, K. T.; Schmitt, K. C.; Baumann, M. H.; Partilla, J. S.; Rothman, R. B.; Katz, J. L. Behavioral, Biological, and Chemical Perspectives on Atypical Agents Targeting the Dopamine Transporter. *Drug Alcohol Depend.* **2015**, *147*, 1–19.
- (29) Tanda, G.; Newman, A. H.; Katz, J. L. Discovery of Drugs to Treat Cocaine Dependence: Behavioral and Neurochemical Effects of Atypical Dopamine Transport Inhibitors. *Adv. Pharmacol.* **2009**, *57*, 253–289.
- (30) Grundt, P.; Kopajtic, T.; Katz, J. L.; Newman, A. H. N-8-Substituted-Benzotropinamine Analogs as Selective Dopamine Transporter Ligands. *Bioorg. Med. Chem. Lett.* **2005**, *15*, 5419–5423.
- (31) Newman, A. H.; Allen, A. C.; Izenwasser, S.; Katz, J. L. Novel 3α-(diphenylmethoxy)tropane analogs: potent dopamine uptake inhibitors without cocaine-like behavioral profiles. *J. Med. Chem.* **1994**, *37*, 2258–2261.
- (32) Newman, A. H.; Kline, R. H.; Allen, A. C.; Izenwasser, S.; George, C.; Katz, J. L. Novel 4'- and 4'', 4''-Substituted-3α-(Diphenylmethoxy)tropane Analogs are Potent and Selective Dopamine Uptake Inhibitors. *J. Med. Chem.* **1995**, *38*, 3933–3940.
- (33) Meltzer, P. C.; Liang, A. Y.; Madras, B. K. The Discovery of an Unusually Selective and Novel Cocaine Analog: Difluoropine. Synthesis and Inhibition of Binding at Cocaine Recognition Sites. *J. Med. Chem.* **1994**, *37*, 2001–2010.
- (34) Zou, M.-F.; Kopajtic, T.; Katz, J. L.; Newman, A. H. Structure-Activity Relationship Comparison of (S)-2β-Substituted 3α-(Bis[4-fluorophenyl]methoxy)tropanes and (R)-2β-Substituted 3β-(3,4-Dichlorophenyl)tropanes at the Dopamine Transporter. *J. Med. Chem.* **2003**, *46*, 2908–2916.

- (35) Zou, M.-F.; Cao, J.; Kopajtic, T.; Desai, R. I.; Katz, J. L.; Newman, A. H. Structure-Activity Relationship Studies on a Novel Series of (S)-2- β -Substituted 3 α -[Bis(4-fluoro- or 4-chlorophenyl)-methoxy]tropane Analogues for In Vivo Investigation. *J. Med. Chem.* **2006**, *49*, 6391–6399.
- (36) Carroll, F. I.; Lewin, A. H.; Boja, J. W.; Kuhar, M. J. Cocaine Receptor: Biochemical Characterization and Structure-Activity Relationships of Cocaine Analogues at the Dopamine Transporter. *J. Med. Chem.* **1992**, *35*, 969–981.
- (37) Katz, J. L.; Izenwasser, S.; Kline, R. H.; Allen, A. C.; Newman, A. H. Novel, 3 α -Diphenylmethoxytropane Analogs: Selective Dopamine Uptake Inhibitors with Behavioral Effects Distinct from those of Cocaine. *J. Pharmacol. Exp. Ther.* **1999**, *288*, 302–315.
- (38) Katz, J. L.; Kopajtic, T.; Agoston, G. E.; Newman, A. H. Effects of N-Substituted Analogs of Benzotropine: Diminished Cocaine-Like Effects in Dopamine Transporter Ligands. *J. Pharmacol. Exp. Ther.* **2004**, *309*, 650–660.
- (39) Woolverton, W. L.; Hecht, G. S.; Agoston, G. E.; Katz, J. L.; Newman, A. H. Further Studies of the Reinforcing Effects of Benzotropine Analogs in Rhesus Monkeys. *Psychopharmacology* **2001**, *154*, 375–382.
- (40) Li, S.-M.; Newman, A. H.; Katz, J. L. Place Conditioning and Locomotor Effects of N-Substituted 4', 4''-Difluorobenzotropine Analogues in Rats. *J. Pharmacol. Exp. Ther.* **2005**, *313*, 1223–1230.
- (41) Ferragud, A.; Velázquez-Sánchez, C.; Canales, J. J. Modulation of Methamphetamine's Locomotor Stimulation and Self-Administration by JHW 007, an Atypical Dopamine Reuptake Blocker. *Eur. J. Pharmacol.* **2014**, *731*, 73–79.
- (42) Desai, R. I.; Grandy, D. K.; Lupica, C. R.; Katz, J. L. Pharmacological Characterization of a Dopamine Transporter Ligand that Functions as a Cocaine Antagonist. *J. Pharmacol. Exp. Ther.* **2014**, *348*, 106–115.
- (43) Velázquez-Sánchez, C.; García-Verdugo, J. M.; Murga, J.; Canales, J. J. The Atypical Dopamine Transport Inhibitor, JHW 007, Prevents Amphetamine-Induced Sensitization and Synaptic Reorganization within the Nucleus Accumbens. *Prog. Neuro-Psychopharmacol. Biol. Psychiatry* **2013**, *44*, 73–80.
- (44) Velázquez-Sánchez, C.; Ferragud, A.; Murga, J.; Cardá, M.; Canales, J. J. The High Affinity Dopamine Uptake Inhibitor, JHW 007, Blocks Cocaine-Induced Reward, Locomotor Stimulation and Sensitization. *Eur. Neuropsychopharmacol.* **2010**, *20*, 501–508.
- (45) Hiranita, T.; Soto, P. L.; Newman, A. H.; Katz, J. L. Assessment of Reinforcing Effects of Benzotropine Analogs and their Effects on Cocaine Self-Administration in Rats: Comparisons with Monoamine Uptake Inhibitors. *J. Pharmacol. Exp. Ther.* **2009**, *329*, 677–686.
- (46) Desai, R. I.; Kopajtic, T. A.; Koffarnus, M.; Newman, A. H.; Katz, J. L. Identification of a Dopamine Transporter Ligand that Blocks the Stimulant Effects of Cocaine. *J. Neurosci.* **2005**, *25*, 1889–1893.
- (47) Tanda, G.; Li, S. M.; Mereu, M.; Thomas, A. M.; Ebbs, A. L.; Chun, L. E.; Tronci, V.; Green, J. L.; Zou, M.-F.; Kopajtic, T. A.; Newman, A. H.; Katz, J. L. Relations Between Stimulation of Mesolimbic Dopamine and Place Conditioning in Rats Produced by Cocaine or Drugs that are Tolerant to Dopamine Transporter Conformational Change. *Psychopharmacology (Berl)* **2013**, *229*, 307–321.
- (48) Kohut, S. J.; Hiranita, T.; Hong, S. K.; Ebbs, A. L.; Tronci, V.; Green, J.; Garcés-Ramírez, L.; Chun, L. E.; Mereu, M.; Newman, A. H.; Katz, J. L.; Tanda, G. Preference for Distinct Functional Conformations of the Dopamine Transporter Alters the Relationship between Subjective Effects of Cocaine and Stimulation of Mesolimbic Dopamine. *Biol. Psychiatry* **2014**, *76*, 802–809.
- (49) Loland, C. J.; Desai, R. I.; Zou, M.-F.; Cao, J.; Grundt, P.; Gerstbrein, K.; Sitte, H. H.; Newman, A. H.; Katz, J. L.; Gether, U. Relationship between Conformational Changes in the Dopamine Transporter and Cocaine-Like Subjective Effects of Uptake Inhibitors. *Mol. Pharmacol.* **2008**, *73*, 813–823.
- (50) Bisgaard, H.; Larsen, M. A.; Mazier, S.; Beuming, T.; Newman, A. H.; Weinstein, H.; Shi, L.; Loland, C. J.; Gether, U. The Binding Sites for Benzotropines and Dopamine in the Dopamine Transporter Overlap. *Neuropharmacology* **2011**, *60*, 182–190.
- (51) Carroll, F. I.; Pawlusch, N.; Kuhar, M. J.; Pollard, G. T.; Howard, J. L. Synthesis, Monoamine Transporter Binding Properties, and Behavioral Pharmacology of a Series of 3 α -(Substituted Phenyl)-2- β -(3'-Substituted Isoxazol-5-yl)tropanes. *J. Med. Chem.* **2004**, *47*, 296–302.
- (52) Cao, J.; Slack, R. D.; Bakare, O. M.; Burzynski, C.; Rais, R.; Slusher, B. S.; Kopajtic, T.; Bonifazi, A.; Ellenberger, M. P.; Yano, H.; He, Y.; Bi, G.-H.; Xi, Z.-X.; Loland, C. J.; Newman, A. H. Novel and High Affinity 2-[(Diphenylmethyl)sulfinyl]acetamide (Modafinil) Analogues as Atypical Dopamine Transporter Inhibitors. *J. Med. Chem.* **2016**, *59*, 10676–10691.
- (53) Berdini, V.; Cesta, M. C.; Curti, R.; D'Anniballe, G.; Di Bello, N.; Nano, G.; Nicolini, L.; Topai, A.; Allegretti, M. A Modified Palladium Catalysed Reductive Amination Procedure. *Tetrahedron* **2002**, *58*, 5669–5674.
- (54) Agoston, G. E.; Wu, J. H.; Izenwasser, S.; George, C.; Katz, J.; Kline, R. H.; Newman, A. H. Novel N-Substituted 3 α -[bis(4'-fluorophenyl)methoxy]tropane Analogues: Selective Ligands for the Dopamine Transporter. *J. Med. Chem.* **1997**, *40*, 4329–4339.
- (55) Zou, M.-F.; Agoston, G. E.; Below, Y.; Kopajtic, T.; Katz, J. L.; Newman, A. H. Enantioselective Synthesis of S-(+)-2- β -Carboalkoxy-3 α -[bis(4-fluorophenyl)methoxy]tropanes as Novel Probes for the Dopamine Transporter. *Bioorg. Med. Chem. Lett.* **2002**, *12*, 1249–1252.
- (56) Staudacher, I.; Schweizer, P. A.; Katus, H. A.; Thomas, D. hERG: Protein Trafficking and Potential for Therapy and Drug Side Effects. *Curr. Opin. Drug Discovery Dev.* **2010**, *13*, 23–30.
- (57) Loland, C. J.; Mereu, M.; Okunola, O. M.; Cao, J.; Prisinzano, T. E.; Mazier, S.; Kopajtic, T.; Shi, L.; Katz, J. L.; Tanda, G.; Newman, A. H. R-Modafinil (Armodafinil): A Unique Dopamine Uptake Inhibitor and Potential Medication for Psychostimulant Abuse. *Biol. Psychiatry* **2012**, *72*, 405–413.
- (58) Abramyan, A. M.; Stolzenberg, S.; Li, Z.; Loland, C. J.; Noé, F.; Shi, L. The Isomeric Preference of an Atypical Dopamine Transporter Inhibitor Contributes to Its Selection of the Transporter Conformation. *ACS Chem. Neurosci.* **2017**, *8*, 1735–1746.
- (59) Sørensen, L.; Andersen, J.; Thomsen, M.; Hansen, S. M.; Zhao, X.; Sandelin, A.; Strømgaard, K.; Kristensen, A. S. Interaction of Antidepressants with the Serotonin and Norepinephrine Transporters Mutational Studies of the S1 Substrate Binding Pocket. *J. Biol. Chem.* **2012**, *287*, 43694–43707.
- (60) Cheng, Y.; Prusoff, W. H. Relationship between the Inhibition Constant (K_i) and the Concentration of Inhibitor Which Causes 50 Per Cent Inhibition (I_{50}) of an Enzymatic Reaction. *Biochem. Pharmacol.* **1973**, *22*, 3099–3108.
- (61) Sherman, W.; Beard, H. S.; Farid, R. Use of an Induced Fit Receptor Structure in Virtual Screening. *Chem. Biol. Drug Des.* **2006**, *67*, 83–84.
- (62) Bochevarov, A. D.; Harder, E.; Hughes, T. F.; Greenwood, J. R.; Braden, D. A.; Philipp, D. M.; Rinaldo, D.; Halls, M. D.; Zhang, J.; Friesner, R. A. Jaguar: A High-Performance Quantum Chemistry Software Program with Strengths in Life and Materials Sciences. *Int. J. Quantum Chem.* **2013**, *113*, 2110–2142.
- (63) Swain, M. Chemicalize.org. *J. Chem. Inf. Model.* **2012**, *52*, 613–615.
- (64) Harder, E.; Damm, W.; Maple, J.; Wu, C.; Reboul, M.; Xiang, J. Y.; Wang, L.; Lupyan, D.; Dahlgren, M. K.; Knight, J. L.; Kaus, J. W.; Cerutti, D. S.; Krilov, G.; Jorgensen, W. L.; Abel, R.; Friesner, R. A. OPLS3: A Force Field Providing Broad Coverage of Drug-Like Small Molecules and Proteins. *J. Chem. Theory Comput.* **2016**, *12*, 281–296.
- (65) Penmatsa, A.; Wang, K. H.; Gouaux, E. X-ray Structure of Dopamine Transporter Elucidates Antidepressant Mechanism. *Nature* **2013**, *503*, 85–90.
- (66) Lomize, M. A.; Lomize, A. L.; Pogozheva, I. D.; Mosberg, H. I. OPM: Orientations of Proteins in Membranes Database. *Bioinformatics* **2006**, *22*, 623–625.

(67) Berendsen, H. J. C.; Postma, J. P. M.; van Gunsteren, W. F.; Hermans, J. Interaction Models for Water in Relation to Protein Hydration. In *Intermolecular Forces: Proceedings of the Fourteenth Jerusalem Symposium on Quantum Chemistry and Biochemistry*; Pullman, B., Ed.; D. Reidel: Holland, 1981; pp 331–342.

(68) Feller, S. E.; Zhang, Y.; Pastor, R. W.; Brooks, B. R. Constant Pressure Molecular Dynamics Simulation: The Langevin Piston Method. *J. Chem. Phys.* **1995**, *103*, 4613–4621.

(69) McGibbon, R. T.; Beauchamp, K. A.; Harrigan, M. P.; Klein, C.; Swails, J. M.; Hernández, C. X.; Schwantes, C. R.; Wang, L.-P.; Lane, T. J.; Pande, V. S. MDTraj: A Modern Open Library for the Analysis of Molecular Dynamics Trajectories. *Biophys. J.* **2015**, *109*, 1528–1532.

(70) Li, S. M.; Kopajtic, T. A.; O'Callaghan, M. J.; Agoston, G. E.; Cao, J.; Newman, A. H.; Katz, J. L. *N*-Substituted Benzotropine Analogs: Selective Dopamine Transporter Ligands with a Fast Onset of Action and Minimal Cocaine-Like Behavioral Effects. *J. Pharmacol. Exp. Ther.* **2011**, *336*, 575–585.

(71) Huang, X. P.; Mangano, T.; Hufeisen, S.; Setola, V.; Roth, B. L. Identification of Human Ether-à-go-go Related Gene Modulators by Three Screening Platforms in an Academic Drug-Discovery Setting. *Assay Drug Dev. Technol.* **2010**, *8*, 727–742.